J. Fluid Mech. (1999), *vol.* 399, *pp.* 117–150. Printed in the United Kingdom

A unified analysis of planar homogeneous turbulence using single-point closure equations

By T. JONGEN[1]† AND T. B. GATSKI[2]

[1] Swiss Federal Institute of Technology, 1015 Lausanne, Switzerland

[2] NASA Langley Research Center, Hampton, VA 23681, USA

(Received 21 January 1998 and in revised form 24 June 1999)

A unified approach for assessing and characterizing both the non-equilibrium and equilibrium states of planar homogeneous flows is analysed within the framework of single-point turbulence closure equations. The underlying methodology is based on the replacement of the modelled evolution equation for the Reynolds stress anisotropy tensor by an equivalent set of three equations for characteristic scalar invariants or state variables. For stress anisotropy evolution equations which use modelled pressure–strain rate correlations that are quasi-linear, this equivalence then leads to an analytic solution for the time evolution of the Reynolds stress anisotropy. With this analysis, the transient system characteristics can be studied, including the dependence on initial states, the occurrence of limit-cycle behaviour, and the system global stability. In the fixed-point asymptotic limit, these results are consistent with and unify previous equilibrium studies, and provide additional information allowing the resolution of some questions that could not be answered in the framework of previous developments. A new result on constraints applicable to the development of realizable pressure–strain rate models is obtained from a re-examination of the stress anisotropy invariant map. With the analytic solution for the transient behaviour, some recent non-equilibrium models, which incorporate relaxation effects, are evaluated in a variety of homogeneous flows in inertial and non-inertial frames.

1. Introduction

The development of higher-order single-point turbulence closure models has evolved from a largely phenomenological process to a more rigorously based mathematical one. While the models still require calibration, the process followed has become more structured and now includes, as required practice, comparative assessment with a class of planar homogeneous flows. These homogeneous flows provide a great deal of insight into key parameters characterizing the turbulence – such as the turbulent stress anisotropy, the production-to-dissipation rate ratio, and the turbulent time scale. While second-moment closures have yet to receive significant attention from industrial users, recent renewed interest in algebraic stress models, which are directly derivable from the Reynolds stress closures, have highlighted the need for a better understanding of the behaviour of the Reynolds stresses at the level of the second-moment closures.

Previous studies on several homogeneous flows (Speziale & Mac Giolla Mhuiris

† Present Address: Unilever Research, PO Box 114, 3130 AC Vlaardingen, The Netherlands.

1989; Speziale, Sarkar & Gatski 1991; Speziale, Abid & Blaisdell 1996) have focused on the fixed points associated with the equilibrium states of the Reynolds stresses in order to assess higher-order models and their ability to reach the correct fixed points. While these fixed-point studies were important and provided useful information concerning the equilibrium state, they were naturally constrained by the lack of information during the transient stage, especially the global stability of the solution, the information on initial conditions, and the existence of limit cycles. Moreover, the complexity of the system seemed to prevent any general assessment concerning the behaviour of the Reynolds stresses in these flows, except in some particular cases.

Increased demands on the predictive capabilities of Reynolds-averaged Navier–Stokes equations for more complex flows has fuelled the need for non-equilibrium models. In the context of homogeneous turbulence, this is directly associated with the transient behaviour of the flow. Thus, a thorough knowledge of the transient dynamics and the subsequent evolution and stability of the fixed points is very useful for the development of improved models. In this study, a unified approach to assessing and characterizing both the non-equilibrium and equilibrium states of planar homogeneous flows is developed within the framework of single-point turbulent closure equations.

The dynamic behaviour of the Reynolds stresses in homogeneous flows is modelled by a tensor evolution equation which can include additional higher-order effects such as dissipation rate anisotropies (Jongen, Mompean & Gatski 1998) and quadratic pressure–strain rate models (Speziale *et al.* 1991). Based on tensor representation theory (Jongen & Gatski 1998*b*), an equivalent set of equations for characteristic scalar invariants, or state variables, is obtained for the Reynolds stress anisotropy tensor evolution, including these additional higher-order effects. An analytic solution is then obtained when a quasi-linear pressure–strain rate model is used and when an isotropic turbulent dissipation rate is assumed for the case of a slowly varying normalised mean strain rate. With this solution, it is now possible to investigate the full dynamic behaviour of the Reynolds stresses, including effects of initial states, early time evolution, limit-cycle occurrence, existence and stability of asymptotic or equilibrium states, and phase-plane analysis.

Fixed-point equilibrium analyses have been used previously in closure model development. Speziale & Mac Giolla Mhuiris (1989) investigated the equilibrium states predicted by both two-equation isotropic eddy viscosity and second-moment closure models for the case of a homogeneous shear flow with and without rotation. A simple quadratic pressure–strain rate correlation model formulation was investigated by Sarkar & Speziale (1990), including the stability of the isotropic fixed point for the return to isotropy case. In their development of a new pressure–strain rate correlation model, Speziale *et al.* (1991) used the fixed points of the dynamical system associated with the evolution of the Reynolds stress anisotropy tensor to assess and calibrate their quadratic (SSG) pressure–strain rate model. Later, an expression for the equilibrium states in plane homogeneous strain was also obtained (Speziale *et al.* 1996) for the quasi-linear version of the SSG model (Speziale *et al.* 1991). More recently, the equilibrium fixed points have been obtained analytically from the asymptotic limit of the Reynolds stress equations (Girimaji 1997; Jongen & Gatski 1998*a*) for planar homogeneous flows in both inertial and non-inertial frames. Unfortunately, both Ying & Canuto (1996) and Girimaji (1996) found that an analysis of the equilibrium state itself was not sufficient to uniquely identify the proper root to select for the production-to-dissipation rate ratio required in their development of an algebraic stress model. However, examining the asymptotic equilibrium limit of the temporal

solution obtained here does yield the proper selection criterion for the production-to-dissipation rate ratio needed. Moreover, the global stability of the solution can now be characterised, including its dependence on the initial state. In addition, it is now possible to demonstrate that the Reynolds stress invariants II_b and III_b are uniquely determined by the model closure coefficients, independent of any explicit dependence on the mean deformation field. Furthermore, this approach yields constraints for the development of more general and realizable pressure–strain rate correlation models. With this extension to a broader range of homogeneous flows and the added insight from the transient dynamics, the present results provide both a broader and more unified description of the equilibrium states attainable by turbulent closures.

The calibration process used for the specification of the closure constants in the turbulence models relys on equilibrium results of homogeneous flows to assess model performance. This includes the numerical simulation or experimental investigation of such flows coupled with a theoretical analysis of the model closure equations. Recently, there has been interest in extending turbulent closure models to include non-equilibrium effects. Such non-equilibrium models when used in conjunction with time-dependent Reynolds-averaged Navier–Stokes (RANS) calculations can be an alternative methodology to large-eddy (LES) or very large-eddy simulations (VLES) (see Ferziger 1993; Speziale 1998). Most commonly used turbulent closures, including the second-moment closures, rely on the previously discussed equilibrium conditions for their calibration (model constant specification) and, to some extent, for their functional form. Turbulent flows with characteristic states that deviate significantly from these conditions cannot be expected to be well represented by these models. The current approaches toward the development of such non-equilibrium models (Speziale & Xu 1996; Speziale 1998; Girimaji 1999*a*) have used relaxation hypotheses for the evolution of the Reynolds stress anisotropies. Inherent limitations of such approaches are demonstrated here. Using the (temporal) analytic solution obtained from the Reynolds stress evolution equations, an algebraic non-equilibrium model is obtained, and is compared with the relaxation models in predicting a variety of temporally evolving homogeneous flows (Leuchter & Benoit 1991; Tanaka *et al.* 1997).

2. Evolution of Reynolds stress anisotropy

Consider incompressible, homogeneous turbulent flow, where the velocity u_i and the kinematic pressure p are decomposed into the ensemble mean and fluctuating parts:

$$u_i = \bar{u}_i + u_i', \qquad p = \bar{p} + p'. \tag{2.1}$$

In homogeneous conditions, the velocity gradients $\partial \bar{u}_i/\partial x_j$ are independent of position. These gradients are also assumed to be independent of time. The Reynolds stress tensor $\tau_{ij} \equiv \overline{u_i' u_j'}$ is a solution of the time evolution equation

$$\dot{\tau}_{ij} = -\tau_{ik}\frac{\partial \bar{u}_j}{\partial x_k} - \tau_{jk}\frac{\partial \bar{u}_i}{\partial x_k} + \Phi_{ij} - \varepsilon_{ij} - 2\Omega_m(e_{mkj}\tau_{ik} + e_{mki}\tau_{jk}), \tag{2.2}$$

which is valid in an arbitrary non-inertial reference frame that can undergo a rotation with angular velocity Ω_m relative to an inertial frame. In (2.2), e_{ijk} is the permutation tensor and

$$\Phi_{ij} = \overline{p'\left(\frac{\partial u_i'}{\partial x_j} + \frac{\partial u_j'}{\partial x_i}\right)}, \qquad \varepsilon_{ij} = 2\nu\overline{\left(\frac{\partial u_i'}{\partial x_k}\frac{\partial u_j'}{\partial x_k}\right)}, \tag{2.3}$$

are the pressure–strain rate correlation and the dissipation rate tensors (where ν is the kinematic viscosity), respectively.

With the turbulent kinetic energy $K \equiv \frac{1}{2}\overline{u_i' u_i'}$, the scalar turbulent dissipation rate $\varepsilon \equiv \frac{1}{2}\varepsilon_{ii}$, and the Reynolds stress anisotropy tensor

$$b_{ij} \equiv \frac{\tau_{ij}}{2K} - \frac{\delta_{ij}}{3}, \tag{2.4}$$

the term Φ_{ij} is modelled in the commonly used second-order closure models in the general form (Speziale *et al.* 1991) as

$$\begin{aligned}\Phi_{ij} = &-\varepsilon\left(C_1^0 + C_1^1\frac{\mathscr{P}}{\varepsilon}\right) b_{ij} + C_2 K S_{ij} + C_3 K\left(b_{ik}S_{kj} + S_{ik}b_{kj} - \tfrac{2}{3}b_{mn}S_{nm}\delta_{ij}\right)\\ &-C_4 K(b_{ik}W_{kj} - W_{ik}b_{kj}) + C_4 K\Omega_m(b_{ik}e_{mkj} - e_{mik}b_{kj})\\ &+C_5\varepsilon\left(b_{ik}b_{kj} - \tfrac{1}{3}b_{mn}b_{nm}\delta_{ij}\right).\end{aligned} \tag{2.5}$$

Above, the strain rate S_{ij} and rotation rate W_{ij} tensors are defined as

$$S_{ij} \equiv \frac{1}{2}\left(\frac{\partial \bar{u}_i}{\partial x_j} + \frac{\partial \bar{u}_j}{\partial x_i}\right), \qquad W_{ij} \equiv \frac{1}{2}\left(\frac{\partial \bar{u}_i}{\partial x_j} - \frac{\partial \bar{u}_j}{\partial x_i}\right), \tag{2.6}$$

and $\mathscr{P} \equiv -\tau_{ij}S_{ij} = -2Kb_{ij}S_{ij}$ is the turbulence production. The coefficients C_1^0, C_1^1, and C_2–C_5 can, in general, be functions of the invariants formed on S_{ij} and W_{ij}. Equation (2.5) can be shown to be the most general form for Φ_{ij} (Speziale *et al.* 1991). For example, the pressure–strain rate model proposed in Speziale *et al.* (1991), which is known as the SSG pressure–strain rate model, gives the following constant values for the coefficients:

$$C_1^0 = 3.4,\ C_1^1 = 1.8,\ C_2 = 0.36,\ C_3 = 1.25,\ C_4 = 0.4,\ C_5 = 4.2. \tag{2.7}$$

A variety of other pressure–strain rate models also fit into the form given in (2.5). For example, the Launder, Reece & Rodi (1975) (LRR) model uses

$$C_1^0 = 3.0,\ C_1^1 = 0,\ C_2 = 0.8,\ C_3 = 1.75,\ C_4 = 1.31,\ C_5 = 0, \tag{2.8}$$

while for the Gibson & Launder (1978) model,

$$C_1^0 = 3.6,\ C_1^1 = 0,\ C_2 = 0.8,\ C_3 = 1.2,\ C_4 = 1.2,\ C_5 = 0, \tag{2.9}$$

and the model proposed by Taulbee (1992) has coefficients defined as

$$C_1^0 = 3.6,\ C_1^1 = 0,\ C_2 = 0.8,\ C_3 = 1.94,\ C_4 = 1.16,\ C_5 = 0. \tag{2.10}$$

It has been known for some time (e.g. Reynolds 1989; Reynolds & Kassinos 1995) that currently used pressure–strain rate correlation models have some inherent deficiencies. Some of these are related to the rapid part of the pressure–strain rate correlation which is composed of a mean velocity gradient contribution and a contribution from the turbulent energy spectrum tensor. In almost all cases, the modelling of the energy spectrum tensor contribution has been solely in terms of the Reynolds stress anisotropy b_{ij}. One of the most fundamental examples of such a deficiency is the case of homogeneous turbulence subjected to mean rotation without strain. Models of the type shown in (2.5) predict no effect of rapid rotation on the second or third invariants of the Reynolds stress anisotropy whereas both simulations and a rapid distortion theory (RDT) analysis (see Mansour, Shih & Reynolds 1991) show an effect through damped oscillatory behaviour of the Reynolds stresses. In a recent low Reynolds number direct numerical simulation of other (weaker) elliptic flows,

Blaisdell & Shariff (1996) have shown that (high Reynolds number) higher-order closure models such as the LRR and SSG models are unable to accurately predict the correct temporal evolution of the turbulent kinetic energy. While the effects of Reynolds number on the simulations are still not clear, these simulations and model comparisons do raise concerns about the ability of single-point closure modelling of elliptic flows. Nevertheless, many shear-dominated flow fields have been and can be accurately computed with such pressure–strain rate models. The analysis to follow explores the behaviour of such models when utilised in single-point, second-moment closures.

The substitution of (2.5) into (2.2) yields the following general evolution equation for the Reynolds stress anisotropy tensor b_{ij}, written in matrix form and in non-dimensionalised variables:

$$\frac{\mathrm{d}}{\mathrm{d}t^*}\boldsymbol{b} = -\frac{1}{\eta}a_0\boldsymbol{b} - a_3\left(\boldsymbol{b}\boldsymbol{S}^* + \boldsymbol{S}^*\boldsymbol{b} - \tfrac{2}{3}\{\boldsymbol{b}\boldsymbol{S}^*\}\boldsymbol{I}\right) + a_2\left(\boldsymbol{b}\boldsymbol{W}^* - \boldsymbol{W}^*\boldsymbol{b}\right) + \frac{1}{\eta}a_4\left(\boldsymbol{b}^2 - \tfrac{1}{3}\{\boldsymbol{b}^2\}\boldsymbol{I}\right) - a_1\boldsymbol{S}^* - \boldsymbol{L}^*, \tag{2.11}$$

where

$$\boldsymbol{S}^* = \boldsymbol{S}/\{\boldsymbol{S}^2\}^{1/2}, \quad \boldsymbol{W}^* = \tilde{\boldsymbol{W}}/\{\boldsymbol{S}^2\}^{1/2}, \quad \boldsymbol{L}^* = \boldsymbol{L}/\{\boldsymbol{S}^2\}^{1/2}, \tag{2.12}$$

$$\eta = \tau\{\boldsymbol{S}^2\}^{1/2}, \quad \zeta = \tau(-\{\tilde{\boldsymbol{W}}^2\})^{1/2}, \quad t^* = t\{\boldsymbol{S}^2\}^{1/2}, \quad \tau = K/\varepsilon. \tag{2.13}$$

The tensor $\tilde{W}_{ij}$ accounts for non-inertial effects

$$\tilde{W}_{ij} = W_{ij} - c_w\Omega_m e_{mij}, \tag{2.14}$$

where $c_w = (C_4 - 4)/(C_4 - 2)$. The following definitions are used for the coefficients in equation (2.11):

$$a_0 = \alpha\frac{\mathscr{P}}{\varepsilon} + \beta, \qquad \alpha = \tfrac{1}{2}C_1^1 + 1, \qquad \beta = \tfrac{1}{2}C_1^0 - 1, \tag{2.15}$$

$$a_1 = \tfrac{1}{2}\left(\tfrac{4}{3} - C_2\right), \qquad a_2 = \frac{(2 - C_4)}{2}, \qquad a_3 = \frac{(2 - C_3)}{2}, \qquad a_4 = \frac{C_5}{2}. \tag{2.16}$$

In the context of equation (2.2), $\boldsymbol{L}(= \boldsymbol{d}/\tau)$ represents the effects of the dissipation rate anisotropy (Jongen *et al.* 1998), with the dissipation rate anisotropy tensor defined as

$$\boldsymbol{d} = d_{ij} = \frac{\varepsilon_{ij}}{2\varepsilon} - \frac{\delta_{ij}}{3}. \tag{2.17}$$

In general, the tensor $\boldsymbol{L}$ can contain additional turbulence anisotropic effects. It will be assumed in this paper that a suitable expression has been provided for $\boldsymbol{L}$ as a tensor function of the tensors $\boldsymbol{S}^*$ and $\boldsymbol{W}^*$, and of the scalars η and ζ.

Equation (2.11) is equivalent to (2.2), but must be supplemented with an equation for the turbulent kinetic energy K

$$\dot{K} = \mathscr{P} - \varepsilon. \tag{2.18}$$

Finally, for closure, an equation for the turbulent dissipation rate ε has to be provided. For instance, it is standard to assume that the evolution of ε is governed by

$$\dot{\varepsilon} = C_{\varepsilon 1}\frac{\varepsilon}{K}\mathscr{P} - C_{\varepsilon 2}\frac{\varepsilon^2}{K}, \tag{2.19}$$

where $C_{\varepsilon 1}$ and $C_{\varepsilon 2}$ are closure constants ($C_{\varepsilon 1} = 1.44$ and $C_{\varepsilon 2} = 1.83$ for the SSG

model, and $C_{\varepsilon 1} = 1.45$ and $C_{\varepsilon 2} = 1.90$ for the Launder *et al.* (1975), and Gibson & Launder (1978) models).

3. Representation and solution method

3.1. *Equivalent scalar representation*

The tensor relation (2.11) governing the evolution of the stress anisotropy cannot be manipulated further because it involves matrix products and their transpose. Even without the quadratic term ($a_4 = 0$), the terms that factor $\boldsymbol{b}$ cannot all be grouped to allow the simple integration of the ordinary differential equation. Moreover, the dependence of the coefficient a_0 upon $\boldsymbol{b}$ through the production-to-dissipation ratio renders equation (2.11) genuinely nonlinear. The following technique, however, transforms the tensor relation into an equivalent system of scalar ordinary differential equations which is better suited for further analysis and which in turn can be solved using the standard tools of the theory of systems of scalar differential equations.

With the evolution of the anisotropy tensor $\boldsymbol{b}$ governed by equation (2.11), the tensor $\boldsymbol{b}$ will depend only on the tensors $\boldsymbol{S}^*$ and $\boldsymbol{W}^*$, as well as on the scalar quantities t^*, η, and ζ. It can be shown in this case that for two-dimensional flows the exact *representation* for the tensor $\boldsymbol{b}$ is given by

$$\boldsymbol{b} = \{\boldsymbol{b}\boldsymbol{S}^*\}\boldsymbol{S}^* + \frac{\{\boldsymbol{b}\boldsymbol{W}^*\boldsymbol{S}^*\}}{\{\boldsymbol{W}^{*2}\}}(\boldsymbol{S}^*\boldsymbol{W}^* - \boldsymbol{W}^*\boldsymbol{S}^*) + 6\{\boldsymbol{b}\boldsymbol{S}^{*2}\}\left(\boldsymbol{S}^{*2} - \tfrac{1}{3}\boldsymbol{I}\right). \tag{3.1}$$

Equation (3.1) is a mathematical identity and shows that if the three scalar invariants $\{\boldsymbol{b}\boldsymbol{S}^*\}$, $\{\boldsymbol{b}\boldsymbol{W}^*\boldsymbol{S}^*\}$, and $\{\boldsymbol{b}\boldsymbol{S}^{*2}\}$ can be determined independently of (3.1), then knowledge of these scalar functions is equivalent to knowing $\boldsymbol{b}$. The interested reader is referred to Jongen & Gatski (1998*b*) for additional details concerning the development of tensorial representations and their analysis. In addition, the representation (3.1) can be used to construct (see Appendix A) the nonlinear term in (2.11),

$$\begin{aligned}\boldsymbol{b}^2 - \tfrac{1}{3}\{\boldsymbol{b}^2\}\boldsymbol{I} = {} & 2\{\boldsymbol{b}\boldsymbol{S}^*\}\{\boldsymbol{b}\boldsymbol{S}^{*2}\}\boldsymbol{S}^* + 2\frac{\{\boldsymbol{b}\boldsymbol{W}^*\boldsymbol{S}^*\}\{\boldsymbol{b}\boldsymbol{S}^{*2}\}}{\{\boldsymbol{W}^{*2}\}}(\boldsymbol{S}^*\boldsymbol{W}^* - \boldsymbol{W}^*\boldsymbol{S}^*) \\ & + \left(\{\boldsymbol{b}\boldsymbol{S}^*\}^2 - 2\frac{\{\boldsymbol{b}\boldsymbol{W}^*\boldsymbol{S}^*\}^2}{\{\boldsymbol{W}^{*2}\}} - 6\{\boldsymbol{b}\boldsymbol{S}^{*2}\}^2\right)\left(\boldsymbol{S}^{*2} - \tfrac{1}{3}\boldsymbol{I}\right),\end{aligned} \tag{3.2}$$

which clearly shows the same tensor function representation as in (3.1), as well as a dependence on the same three scalar invariants. (The derivations in Appendix A originally appeared in Jongen & Gatski (1998*a*), but are reproduced here for completeness.) Independent of the representations shown in (3.1) and (3.2), equations for the three scalar invariants $\{\boldsymbol{b}\boldsymbol{S}^*\}$, $\{\boldsymbol{b}\boldsymbol{W}^*\boldsymbol{S}^*\}$, and $\{\boldsymbol{b}\boldsymbol{S}^{*2}\}$ can be formed (see Appendix B) from the Reynolds stress anisotropy evolution equation given in (2.11). For simplicity in the notation, the following variables are introduced:

$$B_1 = \{\boldsymbol{b}\boldsymbol{S}^*\}, \qquad B_2 = \{\boldsymbol{b}\boldsymbol{W}^*\boldsymbol{S}^*\}, \qquad B_3 = \{\boldsymbol{b}\boldsymbol{S}^{*2}\}, \tag{3.3}$$

and the representation in (3.1) is rewritten as

$$\boldsymbol{b} = B_1\boldsymbol{S}^* - \frac{B_2}{\mathscr{R}^2}(\boldsymbol{S}^*\boldsymbol{W}^* - \boldsymbol{W}^*\boldsymbol{S}^*) + 6B_3\left(\boldsymbol{S}^{*2} - \tfrac{1}{3}\boldsymbol{I}\right), \tag{3.4}$$

where

$$\mathscr{R}^2 = \frac{\zeta^2}{\eta^2} = -\frac{\{\tilde{\boldsymbol{W}}^2\}}{\{\boldsymbol{S}^2\}} = -\{\boldsymbol{W}^{*2}\}. \tag{3.5}$$

The evolution equation (2.11) is, therefore, equivalent to the system of ordinary differential scalar equations in the scalar invariants $\{\boldsymbol{b}\boldsymbol{S}^*\}$, $\{\boldsymbol{b}\boldsymbol{W}^*\boldsymbol{S}^*\}$, and $\{\boldsymbol{b}\boldsymbol{S}^{*2}\}$ that is obtained as shown in Appendix B ((B 5)–(B 7)),

$$\left.\begin{aligned}
\dot{B}_1 &= \left(2\alpha B_1 - \frac{\beta}{\eta}\right) B_1 + 2a_2 B_2 - 2a_3 B_3 + \frac{2a_4}{\eta} B_1 B_3 - a_1 - L_1, \\
\dot{B}_2 &= -a_2 \mathscr{R}^2 B_1 + \left(2\alpha B_1 - \frac{\beta}{\eta}\right) B_2 + \frac{2a_4}{\eta} B_2 B_3 - L_2, \\
\dot{B}_3 &= -\tfrac{1}{3} a_3 B_1 + \left(2\alpha B_1 - \frac{\beta}{\eta}\right) B_3 + \frac{a_4}{6\eta} B_1^2 + \frac{a_4}{3\eta\mathscr{R}^2} B_2^2 - \frac{a_4}{\eta} B_3^2 - L_3,
\end{aligned}\right\} \tag{3.6}$$

where the tensor $\boldsymbol{L}^*$ appears through the invariants

$$L_1 = \{\boldsymbol{L}^*\boldsymbol{S}^*\},\ L_2 = \{\boldsymbol{L}^*\boldsymbol{W}^*\boldsymbol{S}^*\},\ L_3 = \{\boldsymbol{L}^*\boldsymbol{S}^{*2}\}. \tag{3.7}$$

Equation (3.6) is a system of three algebraic ordinary differential equations in the three unknowns B_1, B_2, and B_3, which is quadratic even if $a_4 = 0$ because, as used in obtaining (3.6), a_0 depends on B_1,

$$a_0 = -2\alpha\eta B_1 + \beta. \tag{3.8}$$

Note that the degenerate case of $\eta = 0$ is not considered because either the absence of mean velocity gradients or the absence of a turbulence field would be implied. Of course, no such restrictions apply to ζ, so the case of $\zeta = 0$ is not precluded.

The dynamic system (3.6) is dependent on the initial conditions

$$B_{1,0} = \{\boldsymbol{b}_0\boldsymbol{S}^*\}, \qquad B_{2,0} = \{\boldsymbol{b}_0\boldsymbol{W}^*\boldsymbol{S}^*\}, \qquad B_{3,0} = \{\boldsymbol{b}_0\boldsymbol{S}^{*2}\}, \tag{3.9}$$

where $\boldsymbol{b}_0$ is a given initial anisotropy tensor. The study of the dynamic behaviour of the Reynolds stress tensor governed by the modelled tensor evolution equation (2.11) is now replaced with the study of the system of three scalar ordinary differential equations (3.6).

The present tensor representation technique can be further exploited to characterize the Reynolds stresses. With the formalism introduced in Appendix A,

$$\boldsymbol{b} = \sum_{i=1}^{3} \alpha_i \boldsymbol{T}_i, \tag{3.10}$$

where the scalar coefficients α_i are

$$\alpha_1 = \{\boldsymbol{b}\boldsymbol{S}^*\}, \qquad \alpha_2 = \{\boldsymbol{b}\boldsymbol{W}^*\boldsymbol{S}^*\}/\{\boldsymbol{W}^{*2}\}, \qquad \alpha_3 = 6\{\boldsymbol{b}\boldsymbol{S}^{*2}\}, \tag{3.11}$$

and the tensors $\boldsymbol{T}_i$ are given by

$$\boldsymbol{T}_1 = \boldsymbol{S}^*, \qquad \boldsymbol{T}_2 = \boldsymbol{S}^*\boldsymbol{W}^* - \boldsymbol{W}^*\boldsymbol{S}^*, \qquad \boldsymbol{T}_3 = \boldsymbol{S}^{*2} - \tfrac{1}{3}\boldsymbol{I}, \tag{3.12}$$

the following expressions are obtained:

$$\{\boldsymbol{b}^2\} = \sum_{i=1}^{3}\sum_{j=1}^{3} \alpha_i\alpha_j\{\boldsymbol{T}_i\boldsymbol{T}_j\}, \tag{3.13}$$

and

$$\{\boldsymbol{b}^3\} = \sum_{i=1}^{3}\sum_{j=1}^{3}\sum_{k=1}^{3} \alpha_i\alpha_j\alpha_k\{\boldsymbol{T}_i\boldsymbol{T}_j\boldsymbol{T}_k\}. \tag{3.14}$$

Using the Cayley–Hamilton theorem (Spencer & Rivlin 1959), it is straightforward to show that the 3×3 matrix of invariants $\{\boldsymbol{T}_i \boldsymbol{T}_j\}$ is a diagonal matrix, with $\{\boldsymbol{T}_1 \boldsymbol{T}_1\} = 1$, $\{\boldsymbol{T}_2 \boldsymbol{T}_2\} = 2\mathscr{R}^2$, and $\{\boldsymbol{T}_3 \boldsymbol{T}_3\} = \frac{1}{6}$. The 27 invariants $\{\boldsymbol{T}_i \boldsymbol{T}_j \boldsymbol{T}_k\}$, $(i, j, k = 1, 2, 3)$ have been evaluated in the Appendix A. Thus, using the definitions in (3.3) the resulting expression for the trace of the square and of the cube of the Reynolds stress anisotropy is finally given by

$$\{\boldsymbol{b}^2\} = B_1^2 + \frac{2}{\mathscr{R}^2} B_2^2 + 6B_3^2 \quad \text{and} \quad \{\boldsymbol{b}^3\} = 3B_3 \left[B_1^2 + \frac{2}{\mathscr{R}^2} B_2^2 - 2B_3^2 \right]. \tag{3.15}$$

As a consequence of (3.15), the second and third invariants of the anisotropy, defined as

$$II_b = -\tfrac{1}{2}\{\boldsymbol{b}^2\} \quad \text{and} \quad III_b = \tfrac{1}{3}\{\boldsymbol{b}^3\}, \tag{3.16}$$

are easily evaluated and can be linked together by

$$III_b = -2B_3 \left[II_b + 4B_3^2 \right]. \tag{3.17}$$

These relations are a direct consequence of the representation (3.4) of the Reynolds stress anisotropy tensor, and are therefore always valid, independent of the way the Reynolds stress tensor evolution is modelled. In the current context, the coefficients B_i appearing in (3.15) and (3.17) are the solution of the dynamical system (3.6).

3.2. *Temporal solution*

The system of scalar ordinary differential equations (3.6) with the representation in (3.4) is equivalent to the original tensor evolution equation for the Reynolds stress anisotropy (2.11). However, it has a significant advantage in that it is much more tractable and better suited for analysis than the original tensor equation. Any expression for the extra anisotropy tensor $\boldsymbol{L}$ can be provided which involves the stress anisotropy tensor to any degree of complexity. It then suffices to study the resulting dynamical system (3.6) to have a complete description of the evolution of the Reynolds stress anisotropy tensor (2.11). In the case of quasi-linear pressure–strain rate models, such that $a_4 = 0$ (compare (2.5) with $C_5 = 0$) and no additional anisotropies are included $\boldsymbol{L} = 0$, an explicit solution of the system of ordinary differential equations (3.6) can be obtained in closed form. The term quadratic in the stress anisotropy which is only found in the SSG model can be omitted. This quasi-linear pressure–strain model has been used in the derivation of the Gatski & Speziale (1993) algebraic stress model, and has been found to perform as well as the quadratic form of the model for equilibrium homogeneous flows. The solution procedure for the resulting differential system is not straightforward, and the major steps of its derivation are given in Appendix C. The final expression for the Reynolds stress anisotropy tensor, which is the solution of the modelled evolution equation (2.11) with $a_4 = 0$ and $\boldsymbol{L} = 0$, is rather compact and involves ratios of characteristic functions Ψ_i:

$$\left.\begin{aligned}
B_1(t^*) &= \frac{1}{2\alpha} \left[\frac{\beta}{\eta(t^*)} - \frac{\Psi_3(t^*)}{\Psi_2(t^*)} \right], \\
B_2(t^*) &= \frac{a_2 \mathscr{R}^2}{2\alpha} \left[1 - \frac{\beta}{\eta(t^*)} \frac{\Psi_1(t^*)}{\Psi_2(t^*)} - \frac{1}{\Psi_2(t^*)} \right] + \frac{1}{\Psi_2(t^*)} B_{2,0}, \\
B_3(t^*) &= \frac{a_3}{6\alpha} \left[1 - \frac{\beta}{\eta(t^*)} \frac{\Psi_1(t^*)}{\Psi_2(t^*)} - \frac{1}{\Psi_2(t^*)} \right] + \frac{1}{\Psi_2(t^*)} B_{3,0}.
\end{aligned}\right\} \tag{3.18}$$

The characteristic functions Ψ_i are the fundamental solutions associated with a quadratic nonlinear system of two ordinary differential equations (see Appendix C) and are related by $\Psi_2 = \dot{\Psi}_1$ and $\Psi_3 = \dot{\Psi}_2$,

$$\left.\begin{aligned} \Psi_1(t^*) &= \mathscr{C}\left[\sum_{r=1}^{3} p_r \frac{1}{\lambda_r} \mathrm{e}^{\lambda_r t^*} + p_0(H + H^0)\right], \\ \Psi_2(t^*) &= \mathscr{C}\sum_{r=1}^{3} p_r \mathrm{e}^{\lambda_r t^*}, \quad \Psi_3(t^*) = \mathscr{C}\sum_{r=1}^{3} p_r \lambda_r \mathrm{e}^{\lambda_r t^*}, \end{aligned}\right\} \tag{3.19}$$

where

$$\left.\begin{aligned} H &= \tfrac{2}{3}a_3^2 - 2a_2^2\mathscr{R}^2, \\ H^0 &= 4\alpha(a_2 B_{2,0} - a_3 B_{3,0}), \\ p_r &= [\lambda_r^2 - 2\alpha\lambda_r B_{1,0} - (H + H^0)](\lambda_s - \lambda_q), \quad r = 1, 2, 3, \\ p_0 &= (\lambda_3 - \lambda_2)/\lambda_1 + (\lambda_1 - \lambda_3)/\lambda_2 + (\lambda_2 - \lambda_1)/\lambda_3, \end{aligned}\right\} \tag{3.20}$$

and $\mathscr{C} = [(\lambda_2 - \lambda_1)(\lambda_3 - \lambda_1)(\lambda_3 - \lambda_2)]^{-1}$. In (3.20), the indices q and s are such that $e_{qrs} = -1$. Finally, the parameters λ_r are the eigenvalues that are obtained as roots of the following characteristic cubic polynomial equation:

$$\lambda^3 - \frac{\beta}{\eta}\lambda^2 - (H + 2\alpha a_1)\,\lambda + \frac{\beta}{\eta}H = 0. \tag{3.21}$$

In general, the normalised strain rate depends on the time $\eta = \eta(t^*)$, and its evolution is governed by an additional equation obtained from the evolution equation for K given by (2.18) and from the closure model equation for ε given by (2.19). In this case, the normalised strain rate will be given by the differential equation

$$\frac{\mathrm{d}}{\mathrm{d}t^*}\eta = 2\eta B_1(C_{\varepsilon 1} - 1) + (C_{\varepsilon 2} - 1), \tag{3.22}$$

which must be solved in conjunction with the evolution of the coefficients B_i. However, in the derivation of the explicit solution of the system of ordinary differential equations (3.6), the normalised strain rate η was assumed to vary slowly, $\dot{\eta}/\eta \sim 0$ and $\ddot{\eta}/\eta \sim 0$ (see Appendix C). Before performing the full dynamical analysis of the modelled Reynolds stress evolution in the next section, it will be shown that the present solution is still an extremely good approximation of the differential tensor evolution equation when the normalised strain rate is varying in time. In general, planar homogeneous flows can be described in an appropriate reference frame by the following expression for the velocity gradients tensor (Leuchter & Benoit 1991):

$$\frac{\partial \bar{u}_i}{\partial x_j} = \tfrac{1}{2}\left[(D + \omega)\delta_{i1}\delta_{j2} + (D - \omega)\delta_{i2}\delta_{j1}\right], \tag{3.23}$$

which yields

$$\eta^2 = \tfrac{1}{2}(D\tau)^2, \qquad \zeta^2 = \tfrac{1}{2}\left[(\omega - 2c_w\Omega)\,\tau\right]^2, \tag{3.24}$$

where $D/2$ is the strain rate of the flow, $\omega/2$ is the rotation rate of the flow, and Ω is the angular velocity of the reference frame relative to an inertial framing. As shown in table 1, a wide class of homogeneous flows, both with and without system rotation, can be described in terms of the flow-type parameter $\mathscr{R}$,

$$\mathscr{R}^2 = \left(\frac{\omega}{D} - 2c_w\frac{\Omega}{D}\right)^2. \tag{3.25}$$

Flow	$\lvert\omega/D\rvert$	$\lvert\Omega/D\rvert$	$\lvert\mathscr{R}\rvert$	H^b
Plane shear	1	0	1	−1.19
Plane strain	0	0	0	0.09
Hyperbolic[a]	< 1	0	< 1	> -1.19
Elliptic[a]	> 1	0	> 1	< -1.19
Rotating plane shear	1	0.25, 0.50	0.125, 1.25[b]	0.07, −1.91

[a] See Leuchter & Benoit (1991) for a description of this class of flows.
[b] These values are dependent on the pressure–strain rate model used (SSG model in this case).

TABLE 1. Characterization of common homogeneous turbulent flows.

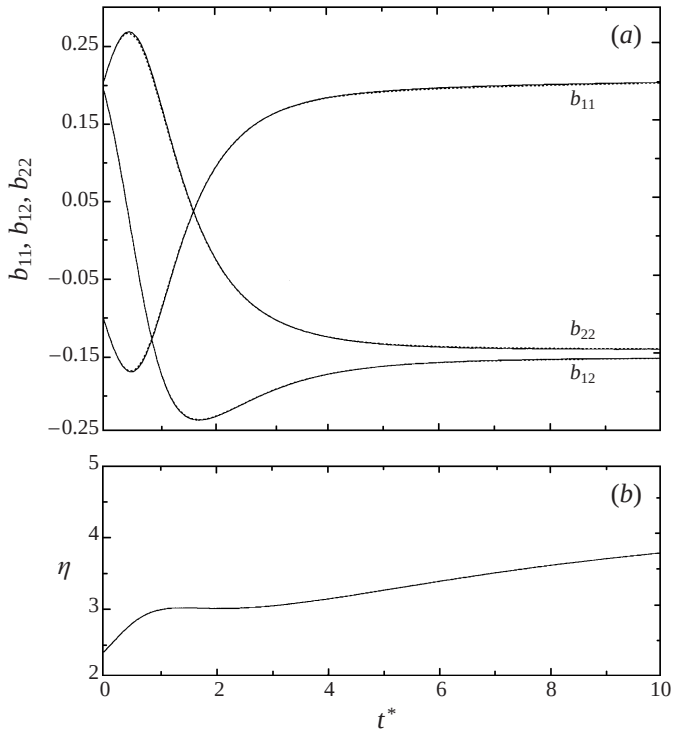

FIGURE 1. Time evolution of the system variables for a homogeneous shear case. The initial conditions are $\eta_0 = 2.39$, $b_{11,0} = -0.1$, $b_{12,0} = 0.2$, $b_{22,0} = 0.2$. ——, Present solution; · · · ·, numerical solution of the differential Reynolds stress equation. (*a*) Evolution of the stress anisotropies; (*b*) evolution of the normalised strain rate.

First, consider a sheared flow ($\mathscr{R} = 1$) in which the turbulent field is subjected to the initial conditions $\eta_0 = 2.39$, $b_{11,0} = -0.1$, $b_{12,0} = 0.2$, $b_{22,0} = 0.2$. This value of the initial normalised strain rate η_0 corresponds to the same initial value of $\varepsilon_0/SK_0 = 0.296$ that was used in the calibration of the SSG model (Speziale *et al.* 1991) for the homogeneous shear flow case, where $S = D = \omega$ is the mean velocity gradient. The initial value for the anisotropy tensor $\boldsymbol{b}_0$ has been chosen arbitrarily, since the present solution is able to account for any initial anisotropy. As time elapses, the anisotropy components and the normalised strain rate evolve towards their asymptotic

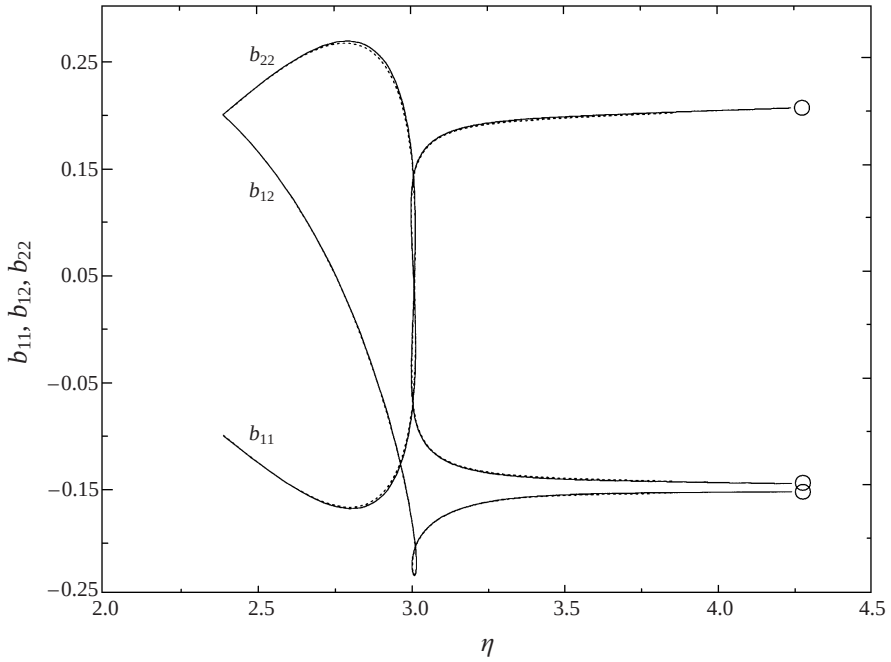

FIGURE 2. Phase-plane evolution for a homogeneous shear case. The initial conditions are $\eta_0 = 2.39$, $b_{11,0} = -0.1$, $b_{12,0} = 0.2$, $b_{22,0} = 0.2$. ——, Present solution; · · · ·, numerical solution of the differential Reynolds stress equation; ○, asymptotic solution.

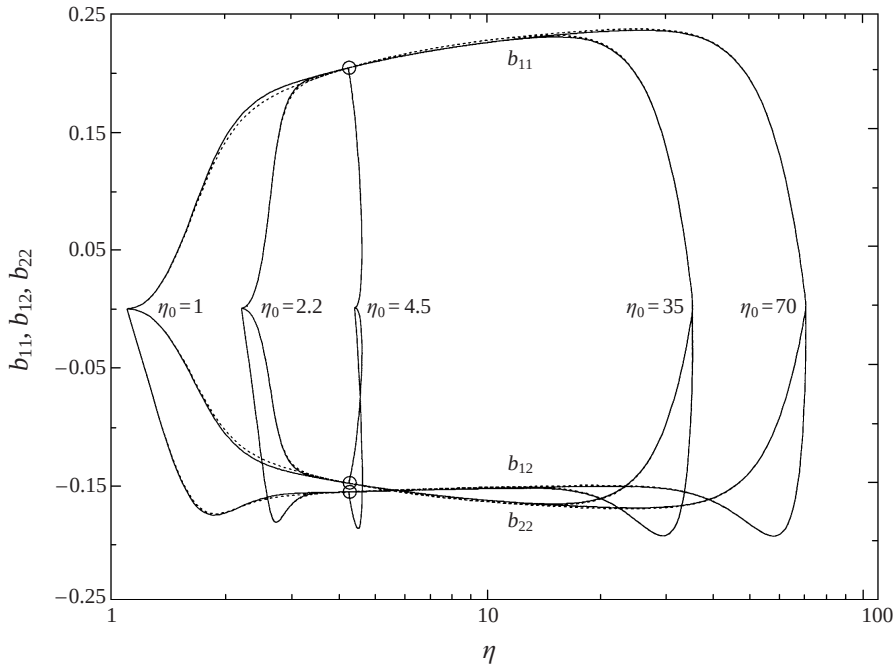

FIGURE 3. Phase-plane evolution for a homogeneous shear case. The initial conditions are $b_{11,0} = b_{12,0} = b_{22,0} = 0$, and different values for η_0 are used, as labelled. ——, Present solution; · · · ·, numerical solution of the differential Reynolds stress equation; ○, asymptotic solution.

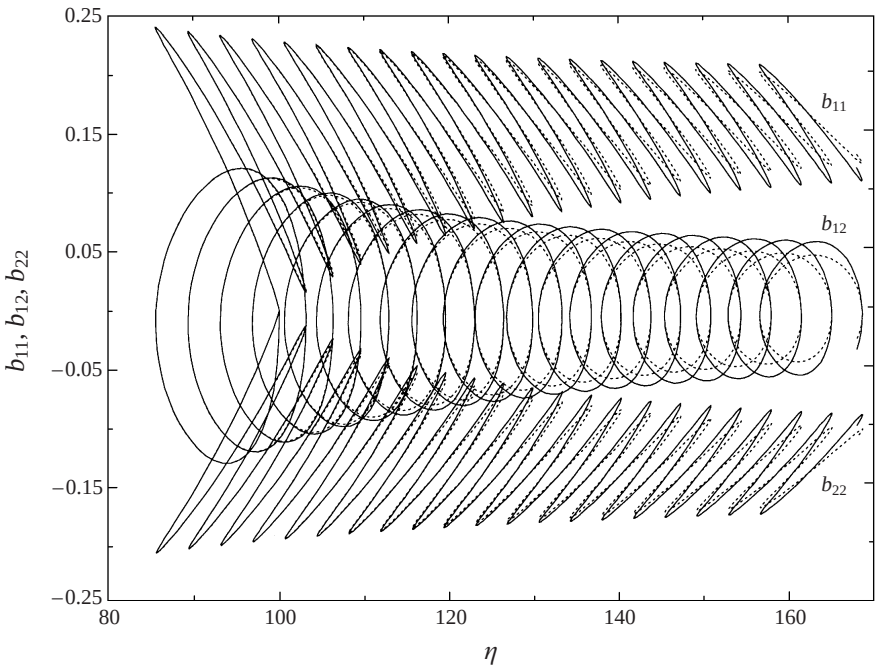

FIGURE 4. Phase-plane evolution for a rotation-dominated flow ($\omega/D = 2$). The initial conditions are $\eta_0 = 100$, $b_{11,0} = b_{12,0} = b_{22,0} = 0$. ——, Present solution; · · ·, numerical solution of the differential Reynolds stress equation.

equilibrium value, as shown in figure 1. From a dynamical system perspective, it is common to represent the evolution of the system variables in the phase plane (η, b_{ij}), as done in figure 2. Clearly, the evolution predicted by the present explicit solution (3.18) is almost indistinguishable from that given by the numerical integration of the differential equation. Moreover, the explicit solution is remarkably close to the solution given by the numerical integration of the differential stress equation over a wide range of initial values η_0, as illustrated in figure 3, where isotropic initial conditions ($b_{ij,0} = 0$) have been used for simplicity. The equilibrium value reached by the system is independent of the initial conditions, and is, of course, the same as the one used for the original calibration of the SSG pressure–strain correlation model (Speziale *et al.* 1991), i.e. $\eta_\infty = 4.26$, $b_{11}^\infty = 0.204$, $b_{12}^\infty = -0.157$, $b_{22}^\infty = -0.149$.

Consider now a rotation-dominated flow, for which $\omega/D = 2$ and $\mathscr{R} = 2$. As discussed further in the next section, this value of the flow parameter $\mathscr{R}$ leads to an oscillatory evolution of the stress anisotropy components, whereas the normalised strain rate grows unbounded. The stability of this class of elliptic flows has been studied extensively using linearised theory (e.g. Cambon, Teissedre & Jeandel 1985; Cambon *et al.* 1994). These and related studies (e.g. Salhi & Lili 1996) have shown that single-point closures in the RDT limit ($1/\eta \to 0$) cannot correctly reproduce the damped oscillatory behaviour of the turbulence. As pointed out in § 2, such deficiencies have been traced to models for the rapid part of the pressure–strain rate correlation which are solely dependent on the stress anisotropy. Starting from an initially isotropic stress field and from an initial (rapid-distortion) value for the normalised strain rate arbitrarily set to $\eta_0 = 100$, the system reaches a limit cycle for the anisotropy components, while the normalised strain rate grows with superimposed oscillations,

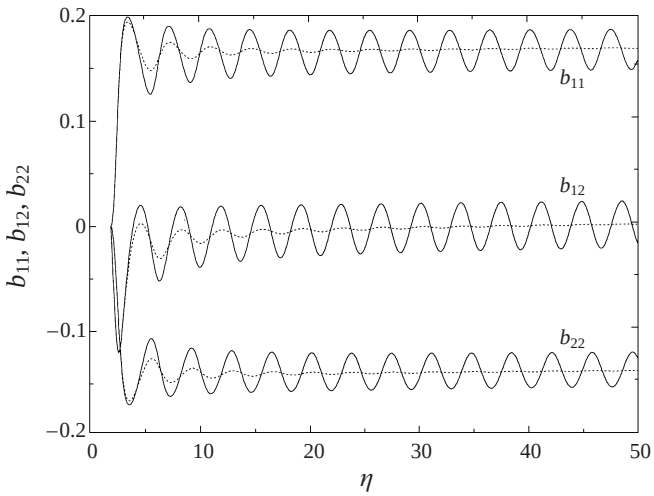

FIGURE 5. Phase-plane evolution for a rotation-dominated flow ($\omega/D = 2$). The initial conditions are $\eta_0 = 2$, $b_{11,0} = b_{12,0} = b_{22,0} = 0$. ——, Present solution; · · ·, numerical solution of the differential Reynolds stress equation.

as shown in figure 4. It is for this most stringent case of limit-cycle behaviour that the assumption of slow variation of the normalised strain rate is the least adequate. The present explicit solution is very accurate in capturing the initial phase of the evolution of the anisotropy, and the period of the oscillations is also very well captured, but the damping of the oscillations, whose rate is proportional to $1/\eta$ (as will be shown in the next section), is not correctly reproduced. For smaller initial normalised strain rate values, the initial damping of the oscillations is much stronger, and the prediction of the amplitude of the oscillations at later times is incorrect, although the period is correctly reproduced, as shown in figure 5, where $\eta_0 = 2$.

These illustrations have shown that even with the assumption on the evolution of the normalised strain rate used in obtaining the explicit time solution of the Reynolds stress anisotropy evolution equation, the predictions are extremely close to the results given by numerical integration of the differential equation in the general case. More importantly, the present solution reproduces all the characteristic dynamical features of the differential system, including the extreme case of limit-cycle behaviour. Even though the differential system may suffer from deficiencies in certain flows (such as the elliptic flows alluded to above), the emphasis here is on the ability of the algebraic stress model to accurately replicate the behaviour of the differential system. These results have shown that the transient solution obtained for the algebraic system can qualitatively and, for the most part, quantitatively replicate the differential system. The study of the properties of the solution (3.18) will therefore provide relevant and accurate information on the modelled behaviour of the Reynolds stresses in planar homogeneous turbulence.

4. Dynamical analysis

4.1. *Transient behaviour*

Equations (3.4) and (3.18) completely determine the solution of the modelled evolution equation for the Reynolds stress anisotropy tensor for all planar homogeneous turbulent flows. Any initial stress anisotropy can be taken into account. The scalars

B_i of the expansion in (3.4) involve ratios of the characteristic functions Ψ_i, which are expressed as the sum of three exponential functions. Because the arguments of the exponentials are the same for all characteristic functions and are given as the roots of the characteristic polynomial (3.21), the dynamical behaviour of the stress anisotropy will essentially be determined by the location of these roots in the complex plane. More precisely, if there is at least one root with a positive real part, the ratios $1/\Psi_2(t^*)$, $\Psi_1(t^*)/\Psi_2(t^*)$, and $\Psi_3(t^*)/\Psi_2(t^*)$ will remain bounded at all times (provided $\Psi_2(t^*) \neq 0$ for all t^*). In this case, the system is stable, and the solution will converge to an asymptotic state (fixed point or limit cycle). It will be seen later that depending on the initial conditions, the characteristic function Ψ_2 may vanish for some time t^*. In this case, the initial condition is outside the basin of attraction, and the solution will diverge. If, on the other hand, all the roots have a negative real part, the ratios $1/\Psi_2(t^*)$ and $\Psi_1(t^*)/\Psi_2(t^*)$ will grow unbounded, corresponding to an unstable system. The dependence of the sign of the roots of the characteristic polynomial upon the system coefficients will therefore be studied in order to characterize the dynamical behaviour of the system. Defining Δ_1 and Δ_2 as

$$\Delta_1 = -\frac{1}{3}\left(H + 2\alpha a_1 + \frac{1}{3}\frac{\beta^2}{\eta^2}\right), \quad \Delta_2 = -\frac{1}{3}\frac{\beta}{\eta}\left(H - \alpha a_1 - \frac{1}{9}\frac{\beta^2}{\eta^2}\right), \tag{4.1}$$

the discriminant of the cubic polynomial equation (3.21) is given by

$$\Delta = \Delta_1^3 + \Delta_2^2, \tag{4.2}$$

and can be rewritten as

$$\Delta = -\frac{1}{27}\left[H\frac{\beta^4}{\eta^4} + (\alpha^2 a_1^2 + 10\alpha a_1 H - 2H^2)\frac{\beta^2}{\eta^2} + (H + 2\alpha a_1)^3\right]. \tag{4.3}$$

Concerning the nature of the roots (denoted λ_1, λ_2, and λ_3), three cases must be distinguished:

(*a*) $\Delta < 0$

The three roots are real, and the characteristic functions Ψ_i are combinations of real exponentials.

(*b*) $\Delta > 0$

Two roots are complex conjugates, for example, $\lambda_2 = d + \mathrm{i}\omega$, $\lambda_3 = d - \mathrm{i}\omega$, and $\lambda_1 = \lambda$. The characteristic functions can then be expressed as

$$\left.\begin{aligned}
\Psi_1(t^*) &= \mathscr{C}'\left[\mathrm{e}^{\lambda t^*} + \mathrm{e}^{\mathrm{d}t^*}(f_{11}\cos\omega t^* + f_{12}\sin\omega t^*) + f_{13}\right], \\
\Psi_2(t^*) &= \mathscr{C}'\left[\lambda\mathrm{e}^{\lambda t^*} + \mathrm{e}^{\mathrm{d}t^*}(f_{21}\cos\omega t^* + f_{22}\sin\omega t^*)\right], \\
\Psi_3(t^*) &= \mathscr{C}'\left[\lambda^2\mathrm{e}^{\lambda t^*} + \mathrm{e}^{\mathrm{d}t^*}(f_{31}\cos\omega t^* + f_{32}\sin\omega t^*)\right],
\end{aligned}\right\} \tag{4.4}$$

where $\mathscr{C}'$ and f_{ij} are parameters obtained directly from (3.19).

(*c*) $\Delta = 0$

The roots are all real, and two of them are equal, for example, $\lambda_2 = \lambda_3 = \lambda$. In this case, $p_1 = 0$, and the third root λ_1 has no effect on the characteristic functions.

At this point, some properties of the roots of a cubic polynomial are recalled:

$$\left.\begin{aligned} &\lambda_1+\lambda_2+\lambda_3=\frac{\beta}{\eta},\\ &\lambda_1\lambda_2\lambda_3=-\frac{\beta}{\eta}H,\\ &\lambda_1\lambda_2+\lambda_2\lambda_3+\lambda_3\lambda_1=-(H+2\alpha a_1). \end{aligned}\right\} \tag{4.5}$$

When $\beta > 0$, the first property pertaining to the sum of the roots in (4.5) implies that at least one root has a positive real part, independent of the value of the other parameters (i.e. H, α, a_1). The case $\beta < 0$ is less straightforward, and properties (4.5) lead to the following sufficient (but not necessary) conditions for having at least one root with a positive real part: $H > 0$ and $2\alpha a_1 > -H$. Otherwise, the roots may all have a negative real part. In summary, at least one root will always have a positive real part when $\beta > 0$, and possibly when $\beta < 0$. As mentioned before, in this case the characteristic functions Ψ_i will grow exponentially, and the system is stable. Moreover, in the case of $\Delta > 0$, the characteristic functions grow with superimposed (damped) oscillations of period $T = 2\pi/\omega$.

The case of a vanishing root is of particular interest. Because of (4.5), one of the roots is zero (e.g. λ_1) if either $H = 0$, $1/\eta = 0$ (RDT limit), or $\beta = 0$. The case $1/\eta = 0$ will be referred here as the RDT limit since $1/\eta \to 0$ yields this limiting behaviour. In the case $H = 0$, $\Delta = -4\alpha^2 a_1^2[\beta^2/(2\eta)^2 + 2\alpha a_1]/27$, and the non-zero roots are given by $\lambda_{2,3} = \beta/(2\eta) \pm ([\beta/(2\eta)]^2 + 2\alpha a_1)^{1/2}$, which can be real or complex. In the case $1/\eta = 0$ or $\beta = 0$, $\Delta = -(H + 2\alpha a_1)^3/27$, and $\lambda_{2,3} = \pm(H + 2\alpha a_1)^{1/2}$. When $H < -2\alpha a_1$, $\Delta > 0$ and the characteristic functions Ψ_2 and Ψ_3 have a purely oscillatory behaviour, while Ψ_1 is increasing as $\int \Psi_2$. The absence of any damping behaviour in this limit is reflected in the fact that the slow part of the pressure–strain correlation model has been effectively removed from the analysis. The Rotta coefficient C_1^0 enters solely through the term β/η in the characteristic equation (3.21) and is effectively lost. The coefficient C_1^1 (which only appears here in the SSG model) only affects the frequency of oscillation. With the primary effects of the slow part of the pressure–strain rate correlation removed, any effects of damping would need to be embedded in the rapid part of the model. As noted previously and shown in Salhi & Lili (1996), current rapid pressure–strain models are unable to display such behaviour.

Interestingly, the fact that the sign of β plays a major role in the stability of the system has already been noticed in Sarkar & Speziale (1990), where it has been shown for a simplified form of the pressure–strain rate model (2.5) with $C_1^1 = C_2 = C_3 = C_4 = 0$, that a stable fixed point existed only when the Rotta coefficient $C_1^0 > 2$ (corresponding to $\beta > 0$, see definition (2.15)). We have shown here that the case $C_1^0 = 2$ is in fact a limit cycle, since the characteristic functions are then purely oscillatory. Abid & Speziale (1993) have also discussed the effect of the Rotta coefficient on the prediction of the equilibrium states in an homogeneous shear flow, and have concluded that the Rotta coefficient C_1^0 should be taken to values slightly higher than 2 in order to obtain the best model predictions, including the logarithmic layer in a channel. It should be noted that virtually all the standard models for the pressure–strain correlation tensor lead to values of $\beta > 0$ (e.g. $\beta = 0.7$ for the SSG model and $\beta = 0.5$ for the Launder *et al.* (1975) model).

Even in the case where at least one root has a positive real part, the system may become unstable, depending on the initial conditions. For a given set of model parameters, the set of all initial conditions $\boldsymbol{b}_0$ that evolve to a bounded asymptotic

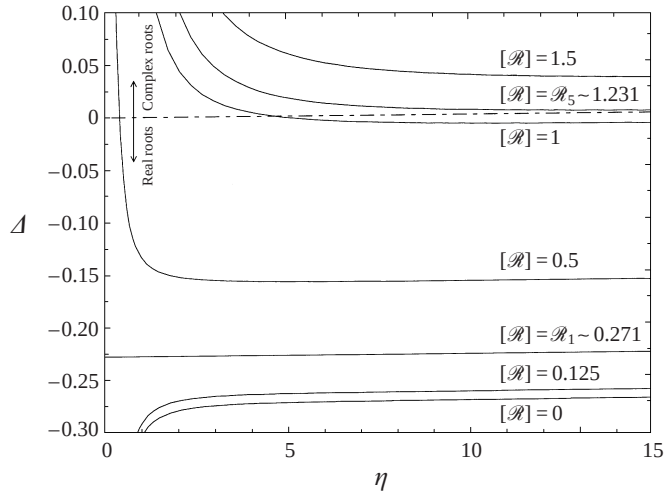

FIGURE 6. Evolution of the discriminant of the cubic characteristic equation as a function of η, for different values of the flow parameter $\mathscr{R}$, as labelled. The closure coefficients are given by the SSG (Speziale *et al.* 1991) model.

state is called the basin of attraction of that asymptotic state. In terms of the present explicit solution in time, the basin of attraction is defined by the set of initial conditions $B_{i,0}$ such that $\Psi_2(t^*) \neq 0$ for all times t^*.

As an illustration, consider the case of a pressure–strain rate model with constant coefficients, whose values are given by the SSG model. Since H is a function of $\mathscr{R}$ (see equation (3.20)), the value of the discriminant Δ will essentially be determined by $\mathscr{R}$ and η. Figure 6 shows the evolution of Δ as a function of η, for different values of the flow parameter $\mathscr{R}$. Three distinct cases can be identified in the figure. For mean flow fields such that $H > 0$, that is, $|\mathscr{R}| < \mathscr{R}_1$, with

$$\mathscr{R}_1 = \frac{a_3}{\sqrt{3}a_2} \tag{4.6}$$

($\mathscr{R}_1 = 0.271$ for the SSG model), the discriminant is always negative, and the three roots are always real, for any value of η. For values of H such that $-2\alpha a_1 < H < 0$, that is $\mathscr{R}_1 < |\mathscr{R}| < \mathscr{R}_2$, with

$$\mathscr{R}_2 = \frac{1}{a_2}\left(\tfrac{1}{3}a_3^2 + \alpha a_1\right)^{1/2} \tag{4.7}$$

($\mathscr{R}_2 = 1.231$ for the SSG model), the roots will have a different nature depending on the magnitude of η, and the evolution of the stress anisotropy will contain an oscillatory component for sufficiently small values of the normalised strain rate. Finally, for values $H < -2\alpha a_1$, that is, $|\mathscr{R}| > \mathscr{R}_2$, the discriminant is now always positive, and the evolution of the stress anisotropy components will be composed of damped oscillations. Once again note that only in the limit $1/\eta = 0$ is the effects of damping removed from the algebraic system; otherwise, the damping effect of the slow part of the pressure–strain rate model is retained from the differential system.

4.2. *Asymptotic states*

It has been shown in the previous subsection that when $\beta > 0$, the characteristic functions Ψ_i are always increasing, except when $1/\eta = 0$. For $1/\eta \neq 0$, when the

effect of the initial conditions has vanished, the exponential that corresponds to the root with the largest real part becomes dominant, and the ratios of the characteristic functions converge to the values

$$\left[\frac{\Psi_3(t^*)}{\Psi_2(t^*)}\right]_\infty = \lim_{t^*\to\infty}\frac{\Psi_3(t^*)}{\Psi_2(t^*)} = \lambda_\infty, \quad \left[\frac{\Psi_1(t^*)}{\Psi_2(t^*)}\right]_\infty = \lim_{t^*\to\infty}\frac{\Psi_1(t^*)}{\Psi_2(t^*)} = \frac{1}{\lambda_\infty}, \tag{4.8}$$

where

$$\lambda_\infty = \max_{r=1,2,3} Re\,(\lambda_r). \tag{4.9}$$

The asymptotic values of the coefficients B_i are given by

$$\left.\begin{aligned} B_1^\infty &= -\frac{\lambda_\infty}{2\alpha}\left(1-\frac{\beta}{\lambda_\infty\eta_\infty}\right), \\ B_2^\infty &= \frac{a_2\mathscr{R}^2}{2\alpha}\left(1-\frac{\beta}{\lambda_\infty\eta_\infty}\right) = -\frac{a_2\mathscr{R}^2}{\lambda_\infty}B_1^\infty, \\ B_3^\infty &= \frac{a_3}{6\alpha}\left(1-\frac{\beta}{\lambda_\infty\eta_\infty}\right) = -\frac{a_3}{3\lambda_\infty}B_1^\infty, \end{aligned}\right\} \tag{4.10}$$

where η_∞ is the equilibrium value achieved by the normalised strain rate. By definition,

$$\frac{\mathscr{P}}{\varepsilon} = -2\{\boldsymbol{bS}^*\}\eta = -2\eta B_1, \tag{4.11}$$

and the asymptotic state therefore verifies the following interesting property:

$$\lambda_\infty\eta_\infty = \alpha\left(\frac{\mathscr{P}}{\varepsilon}\right)_\infty + \beta = a_0, \tag{4.12}$$

obtained by using (4.10). Note that the values of the coefficients α, β, and a_i refer, in the general case of variable closure coefficients, to the asymptotic value of these coefficients. The equilibrium value of the production-to-dissipation ratio $(\mathscr{P}/\varepsilon)_\infty$ is determined by the K and ε evolution equations. For the standard approach where equations (2.18) and (2.19) are used, this value is given by

$$\left(\frac{\mathscr{P}}{\varepsilon}\right)_\infty = \frac{C_{\varepsilon 2}-1}{C_{\varepsilon 1}-1}. \tag{4.13}$$

Relationship (4.12) linking together the equilibrium values of the production-to-dissipation ratio, the characteristic eigenvalue, and the normalised strain rate, can be taken into account in order to simplify the characteristic polynomial equation (3.21), which can then be recast as a relation giving the value of η_∞ in terms of $(\mathscr{P}/\varepsilon)_\infty$ and $\mathscr{R}$:

$$\begin{cases} \dfrac{1}{\eta_\infty^2} = 2\dfrac{a_1}{a_0}\left(\dfrac{\mathscr{P}}{\varepsilon}\right)_\infty^{-1} + \dfrac{1}{a_0^2}H, & \text{for } -\mathscr{R}_{\lim} < \mathscr{R} < \mathscr{R}_{\lim}, \\ \dfrac{1}{\eta_\infty^2} = 0, & \text{otherwise} \end{cases} \tag{4.14}$$

where

$$\mathscr{R}_{\lim} = \frac{1}{a_2}\left[\tfrac{1}{3}a_3^2 + a_0a_1\left(\frac{\mathscr{P}}{\varepsilon}\right)_\infty^{-1}\right]^{1/2}. \tag{4.15}$$

This relationship between the equilibrium value for the production-to-dissipation ratio $(\mathscr{P}/\varepsilon)_\infty$, the equilibrium normalised strain rate η_∞, and the flow-type parameter $\mathscr{R}$ has to be satisfied by any planar homogeneous flow described by the Reynolds stress model equation (2.2), as discussed by Jongen & Gatski (1998*a*). In fact, equation (4.14) is the rigorous generalization of the expression found by Speziale & Mac Giolla Mhuiris (1989) (see their equation (73)) for the equilibrium states in the case of a homogeneous shear flow with and without rotation, and by Speziale *et al.* (1996) (see their equation (22)) in the plane homogeneous strain case. As discussed in the previous subsection, the value $\Delta = 0$ divides the plane $(\mathscr{R}, \eta)$ into two regions in which the Reynolds stress components have distinctly different behaviours in time. These regions are illustrated in figure 7, where the solid lines are determined by the locus of points $(\mathscr{R}, \eta)$ such that $\Delta = 0$ in the SSG pressure–strain rate case. Figure 7 also shows the locus of asymptotic solutions $1/\eta_\infty$ as a function of $\mathscr{R}$, as defined by (4.14). (Note the dashed line in figure 7.) The symbols correspond to several planar homogeneous flows. (See table 1.) Because for a given planar homogeneous flow the value of the flow parameter $\mathscr{R}$ is fixed, the system will evolve along vertical lines in figure 7. For values of $(\mathscr{R}, \eta)$ situated in region I of figure 7, the roots of the characteristic polynomial are real, and the Reynolds stress components converge to the asymptotic solution as ratios of real exponentials. For example, planar strain flows and rotating shear flows with $\Omega/D = 0.25$ will always have an evolution that is characterised by the ratio of growing exponentials, for any initial condition on the anisotropy $\boldsymbol{b}_0$ in the basin of attraction, or on the normalised strain rate η_0. Points in region II have a time evolution with a damped oscillatory character, and the asymptotic state is a spiral sink. The rate of damping of the oscillations is proportional to $1/\eta$, with no damping at all when $1/\eta = 0$ (RDT limit). For example, a shear flow with high rotation ($\Omega/D = 0.5$) is such that $|\mathscr{R}| > \mathscr{R}_2$, and the stress components will evolve to their asymptotic value with damped oscillations. Note that for the homogeneous shear case ($\mathscr{R}_1 < |\mathscr{R}| < \mathscr{R}_2$), the two types of evolution can be experienced depending on the value of η. As already mentioned, for $|\mathscr{R}| > \mathscr{R}_{\lim}$, the asymptotic solution for the normalised strain rate is $1/\eta_\infty = 0$, and the solution is purely oscillatory, i.e. a limit cycle is reached.

For values of the flow parameter $\mathscr{R}$ outside the range $[-\mathscr{R}_{\lim}, \mathscr{R}_{\lim}]$, the asymptotic value of the normalised strain rate is $1/\eta_\infty = 0$, and the representation coefficients given by (4.10) are

$$B_1^\infty = -\lambda_\infty/(2\alpha), \qquad B_2^\infty = a_2\mathscr{R}^2/(2\alpha), \qquad B_3^\infty = a_3/(6\alpha). \tag{4.16}$$

However, as shown before, for $1/\eta = 0$, the solution reaches a limit cycle for the anisotropy, and no fixed-point asymptotic state exists. The solution (4.16) is, therefore, spurious because the real behaviour of the anisotropy is purely oscillatory in time.

In previous studies (Ying & Canuto 1996; Girimaji 1996), an expression equivalent to (4.10) was obtained from a direct analysis of the asymptotic state of (2.11). Written in the present formalism, the asymptotic value for the representation coefficient B_1^∞ was obtained from the roots of a cubic polynomial in B_1^∞,

$$4\alpha^2(B_1^\infty)^3 - 4\alpha\frac{\beta}{\eta}(B_1^\infty)^2 + \left(\frac{\beta^2}{\eta^2} - H - 2\alpha a_1\right) B_1^\infty + \frac{\beta}{\eta}a_1 = 0, \tag{4.17}$$

which led to the problem of choosing one of the three roots so that the correct value of B_1^∞ was retained. This question could not be rigorously answered, and the selection of the proper root was done on the basis of continuity arguments (Ying & Canuto 1996; Girimaji 1996). With the present dynamic approach of the Reynolds

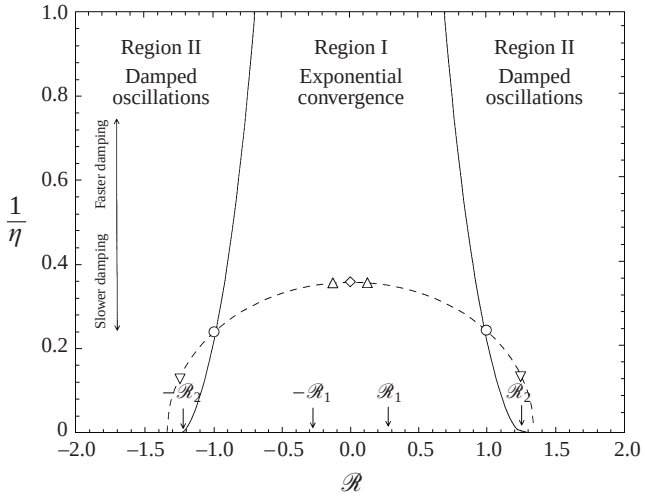

FIGURE 7. Time-evolution types for the Reynolds stress tensor in the $(\mathscr{R}, 1/\eta)$-plane. ———, Locus of points such that $\Delta = 0$; — — —, locus of equilibrium points $1/\eta_\infty$ as function of $\mathscr{R}$; ○, plane shear; ◇, plane strain; △ and ▽, rotating plane shear $|\Omega/D| = 0.25$ and 0.50, respectively. The closure coefficients are given by the SSG (Speziale *et al.* 1991) model.

stress equation, the proper choice for the roots in (4.17) is obvious and is based on the limit of a dynamical process. Clearly, the correct root is the one that controls the asymptotic behaviour of the system (i.e. λ_∞). In terms of B_1^∞, B_1^∞ must be taken as the root in (4.17) that has *the lowest real part*.

Replacing in (3.15) the coefficients B_i by their expression (4.10), the asymptotic value of the Reynolds stress anisotropy invariants is given by

$$II_b^\infty = -\frac{1}{8\alpha^2}\left(1 - \frac{\beta}{\lambda_\infty \eta_\infty}\right)^2 \left(\lambda_\infty^2 + H + 4a_2^2\mathscr{R}^2\right), \tag{4.18}$$

and

$$III_b^\infty = \frac{a_3}{24\alpha^3}\left(1 - \frac{\beta}{\lambda_\infty \eta_\infty}\right)^3 \left(\lambda_\infty^2 - H + \tfrac{4}{9}a_3^2\right). \tag{4.19}$$

Using property (4.12), the second and third invariants are easily expressed as

$$II_b^\infty = -\frac{1}{4a_0}\left(\frac{\mathscr{P}}{\varepsilon}\right)_\infty^2 \left[a_1\left(\frac{\mathscr{P}}{\varepsilon}\right)_\infty^{-1} + \frac{2}{3}\frac{a_3^2}{a_0}\right], \tag{4.20}$$

and

$$III_b^\infty = -\frac{a_3}{12a_0^2}\left(\frac{\mathscr{P}}{\varepsilon}\right)_\infty^3 \left[a_1\left(\frac{\mathscr{P}}{\varepsilon}\right)_\infty^{-1} + \frac{2}{9}\frac{a_3^2}{a_0}\right], \tag{4.21}$$

which leads to the following relation between the second and third invariants:

$$III_b^\infty = -\frac{a_3}{3a_0}\left(\frac{\mathscr{P}}{\varepsilon}\right)_\infty \left[II_b^\infty + \frac{a_3^2}{3a_0^2}\left(\frac{\mathscr{P}}{\varepsilon}\right)_\infty^2\right]. \tag{4.22}$$

This fundamental relation is satisfied by the asymptotic states of *any* Reynolds stress closure using the quasi-linear pressure–strain rate correlation model (2.5) in a planar homogeneous flow. We have therefore proven the following result: *In any*

planar homogeneous flow, the equilibrium states predicted by the Reynolds stress model equations using the quasi-linear form of the pressure–strain rate (2.5) are such that the second and third invariants II_b^∞ and III_b^∞ do not depend explicitly on $\{\boldsymbol{S}^2\}$ and $\{\tilde{\boldsymbol{W}}^2\}$ (i.e. the flow field), and depend only on the pressure–strain rate model coefficients C_1^0, C_1^1, C_2, C_3, and on the equilibrium value of the production-to-dissipation rate ratio $\left(P/\varepsilon\right)_\infty$ (i.e. the closure coefficients $C_{\varepsilon 1}$ and $C_{\varepsilon 2}$ of the ε evolution equation). In other words, current pressure–strain rate models with constant closure coefficients will predict the same anisotropy invariants in a homogeneous shear as in a homogeneous strain, for instance. Note also that the coefficient a_2 (thus C_4) does not play any role in the determination of II_b^∞ and III_b^∞. Removing the effects of $\tilde{\boldsymbol{W}}$ on the equilibrium system is a deficiency of current Reynolds stress closures and specifically the rapid part of the pressure–strain rate correlation model. This deficiency was highlighted previously for the case of rapidly rotating turbulence (Reynolds 1989), but through this analysis is also shown to occur outside the RDT range for the invariants II_b^∞ and III_b^∞.

In order to improve Reynolds stress model predictions, a number of recent studies (Speziale 1998; Girimaji 1999*b*) have proposed to sensitize the pressure–strain rate correlation coefficients to the flow-field invariants $\{\boldsymbol{S}^2\}$ and $\{\tilde{\boldsymbol{W}}^2\}$, and to the turbulence time scale τ, which is equivalent to assuming that

$$C_1^0 = C_1^0(\eta,\zeta), \qquad C_1^1 = C_1^1(\eta,\zeta), \qquad C_i = C_i(\eta,\zeta), \quad i = 2,\ldots,5. \tag{4.23}$$

Speziale (1998) modified the $C_i(\eta,\zeta)$ coefficients indirectly by using a Padé approximation extension of the original Gatski & Speziale (1993) explicit algebraic stress model which satisfies the RDT limiting behaviour of homogeneous shear flow. Girimaji (1999*b*) developed closure values for both $C_2(\eta,\zeta)$ and $C_4(\eta,\zeta)$ using RDT and equilibrium results for homogeneously strained turbulence, and the equilibrium behaviour of the bifurcation points for elliptic flows, respectively. Since equations (4.20) and (4.21) establish the causality between the model coefficients in the pressure–strain rate correlation model and the invariants of the asymptotic state of the anisotropy for planar homogeneous turbulence, it is now possible to develop improved pressure–strain rate correlation models that lead to results closer to the observed equilibrium behaviour by analysing the response of the stress anisotropy to changes in the closure coefficients. One other implication of the above relationships is that it is now possible to assess the realizability of Reynolds stress models from a new perspective, and to derive new constraints on the closure coefficients. The constraint of realizability requires that a Reynolds stress model yields non-negative component energies in all turbulent flows, with the Schwarz inequality satisfied for each off-diagonal component of the Reynolds stress tensor (Schumann 1977). It can be shown (Lumley 1978) that in order to be realizable, the second and third invariants of the stress anisotropy tensor must be located in the region of the invariant plane $(III_b, -II_b)$ delimited by the curves

$$-II_b = \tfrac{1}{9} + 3III_b \quad \text{and} \quad -II_b = 3\left|\frac{III_b}{2}\right|^{2/3} \tag{4.24}$$

with $-1/108 \leqslant III_b \leqslant 2/27$. The standard strategy developed in previous studies (Schumann 1977; Lumley 1978; Speziale, Abid & Durbin 1994) has been to impose conditions on the time derivative $\mathrm{D}\tau_{ij}/\mathrm{D}t$ of the Reynolds stress tensor in order to prevent the model from predicting non-realizable states. In this case, the behaviour of the dynamical system was modified by imposing restrictions on the evolution pattern of the Reynolds stresses, and realizability was generally enforced by implementing

weak and strong realizability constraints (Speziale *et al.* 1994) that are activated as soon as the Reynolds stress tensor reaches one of the boundaries of the realizability domain. With the present methodology giving explicitly and analytically the relation between the equilibrium states and the model parameters, it is possible to directly impose realizability conditions on the Reynolds stresses themselves, and full control of the behaviour of the model can be obtained, even when far from the realizability domain boundaries. The sensitivity of the equilibrium values to variations in the model coefficients is illustrated in the invariant maps given in figure 8.

From the expressions (4.20) and (4.21) of the stress invariants, it is possible to further derive algebraic constraints on the closure coefficients, and to determine ranges in which these coefficients must lie in order to guarantee the realizability of the turbulence predictions. The relationships (4.20) and (4.21) between the stress anisotropy invariants and the closure coefficients can be rewritten as a function of the following two groups of coefficients only:

$$X = \frac{a_3^2}{a_0 a_1}\left(\frac{\mathscr{P}}{\varepsilon}\right)_\infty \quad \text{and} \quad Y = \frac{a_3}{a_1}, \tag{4.25}$$

and thus

$$II_b^\infty = -\frac{1}{12}\frac{X}{Y^2}(2X+3), \tag{4.26}$$

and

$$III_b^\infty = \frac{1}{108}\frac{X^2}{Y^3}(2X+9). \tag{4.27}$$

To each point in the invariant plane $(III_b, -II_b)$ corresponds at least one point in the (X, Y)-plane. There will therefore exist a region of the (X, Y)-plane where the corresponding turbulence state is realizable. This is shown in figure 9, where the shaded area in the (X, Y)-plane is the realizable region. For any choice of pressure–strain rate correlation model coefficients, the corresponding point in the (X, Y)-plane must lie in the shaded area for the turbulence predictions to be realizable. The boundaries of these regions correspond to the boundaries of the invariant map. The curves Y_1, Y_2, and Y_3, delimiting the realizable region, are defined by

$$\left.\begin{aligned} Y_1 &= X, && X \leqslant -3 \ \text{ and } \ X \geqslant \tfrac{3}{2}, \\ Y_2 &= -\tfrac{1}{2}X - \tfrac{1}{2}\left[3X(X+3)\right]^{1/2}, && X \geqslant 0, \\ Y_3 &= -\tfrac{1}{2}X + \tfrac{1}{2}\left[3X(X+3)\right]^{1/2}, && X \leqslant -3 \ \text{ and } \ 0 \leqslant X \leqslant \tfrac{3}{2}. \end{aligned}\right\} \tag{4.28}$$

With this diagram, it is now easy to design new pressure–strain rate correlation coefficients that guarantee realizability by forming the groups X and Y, and checking that the points lie in the realizable region. Of course, other considerations may be taken into account in the design of improved pressure–strain rate correlation models; the analysis provided here can be used in conjunction with any other design methodology in order to obtain well-behaved Reynolds stress closure models.

5. Non-equilibrium models

In the context of non-equilibrium turbulence modelling, it is essential that the closure be able to replicate the evolution of the individual stress components. It has been shown (Mansour *et al.* 1991; Speziale *et al.* 1996; Salhi & Lili 1996; Blaisdell & Shariff 1996) that in homogeneous flows where $\mathscr{R} > 1$ (elliptic flow), single-point

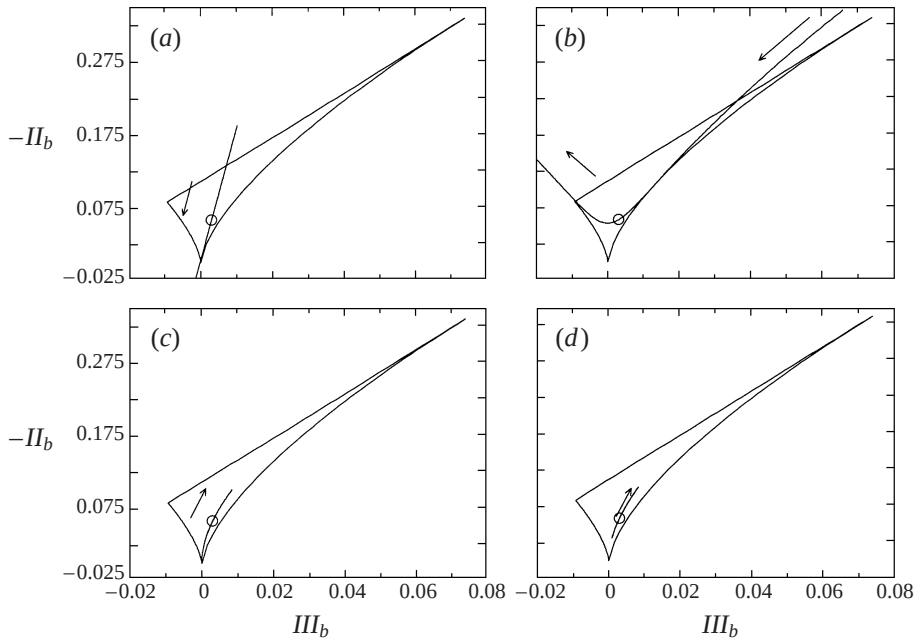

FIGURE 8. Equilibrium values in the invariant map $(III_b, -II_b)$ as a function of the closure coefficients C_1^0, C_1^1, C_2, C_3, and the ratio $\mathscr{P}/\varepsilon$ in (2.5). The arrows indicate the direction of increase of the parameter value. (*a*) Variation of C_2 from −2 to 2; (*b*) variation of C_3 from −4 to 6; (*c*) variation of $\mathscr{P}/\varepsilon$ from 0 to 20; (*d*) Variation of C_0^1 or C_1^1 from 0 to 10. ○, Location corresponding to the SSG (Speziale *et al.* 1991) model.

closures are unable to capture the correct dynamic behaviour of the turbulence statistics. In inhomogeneous flows, such elliptic flow regions can be embedded within the flow domain and be an inherent source of error between model predictions and measurements (or simulation). Outside this region $\mathscr{R} \leqslant 1$ single-point closures are able to predict a wide variety of flows and can be extended to the more complex non-equilibrium flows.

The most sophisticated level of single-point closure modelling is the differential Reynolds stress model, where an evolution equation is solved for each individual Reynolds stress component (see equation (2.11)). The present explicit time-dependent solution of (2.11) allows us to develop a non-equilibrium model in the framework of the more economical two-equation turbulence closures. In this case, the evolution equations (2.18) and (2.19) for the scale-determining quantities K and ε are integrated in time, with the Reynolds stress tensor determined at every instant by the relations (3.4) and (3.18).

The majority of previously proposed non-equilibrium models (Speziale & Xu 1996; Girimaji 1999*a*) are based on a relaxation time approximation around a prescribed equilibrium state. This can be expressed as

$$\frac{\mathrm{d}\boldsymbol{b}}{\mathrm{d}t^*} = -\frac{C}{\eta}(\boldsymbol{b} - \boldsymbol{b}^\infty), \tag{5.1}$$

where $\boldsymbol{b}^\infty$ is the given equilibrium state and C is a relaxation coefficient. The general solution of (5.1) is given by

$$\boldsymbol{b}(t^*) = \left(1 - \exp\left(-\int_0^{t^*} (C/\eta)\,\mathrm{d}s\right)\right)\boldsymbol{b}^\infty + \boldsymbol{b}_0 \exp\left(-\int_0^{t^*} (C/\eta)\,\mathrm{d}s\right). \tag{5.2}$$

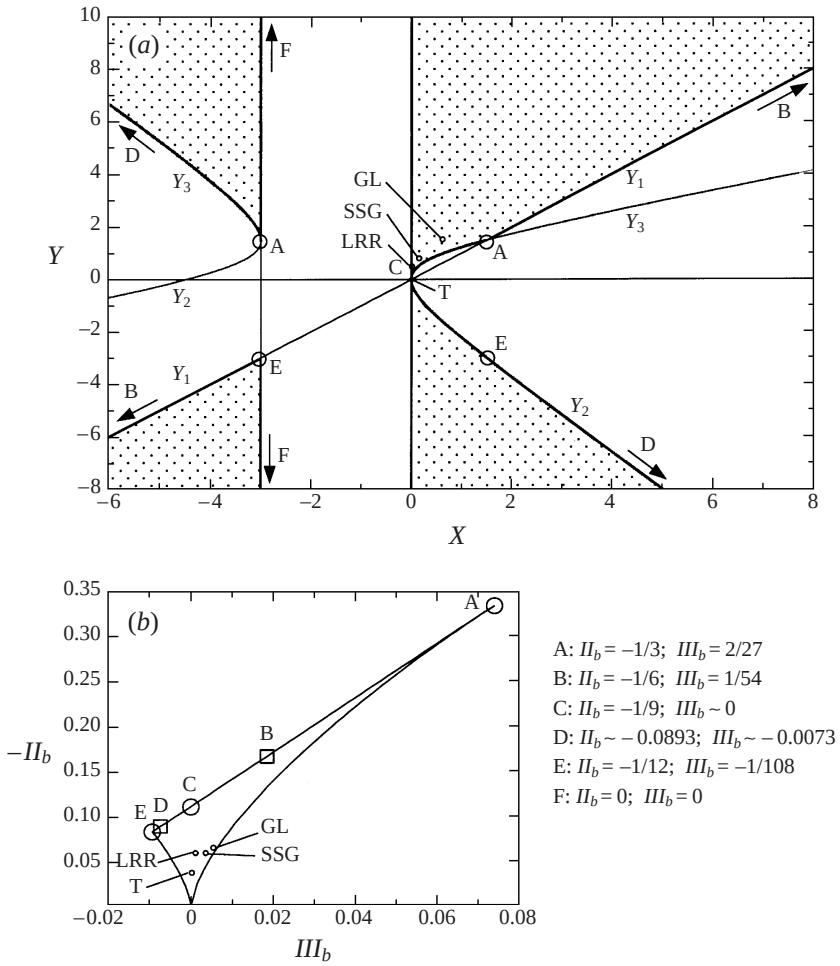

FIGURE 9. (*a*) Map in the plane (X, Y) of the domain in which the predicted turbulence is realizable. (*b*) Corresponding points in the invariant map $(III_b, -II_b)$. Equilibrium points for different pressure–strain rate correlation models are also included: SSG, Speziale *et al.* (1991); LRR, Launder *et al.* (1975); GL, Gibson & Launder (1978); T, Taulbee (1992).

Although this formulation takes into account the initial conditions $\boldsymbol{b}_0$, the evolution toward equilibrium is accomplished in a simplistic way through the multiplication by a scalar, which imposes a strong restriction on the evolution of the individual anisotropy components. Due to the isotropic scaling of the final state, the anisotropy components will all evolve in a similar way to equilibrium. For instance, in the case of isotropic initial conditions, each stress anisotropy component will evolve at the same rate to the asymptotic value,

$$\frac{b_{11}}{b_{11}^{\infty}} = \frac{b_{12}}{b_{12}^{\infty}} = \cdots = 1 - \exp\left(-\int_0^{t^*} (C/\eta)\,\mathrm{d}s\right). \tag{5.3}$$

In order to compare the performance of the present non-equilibrium model and the relaxation models, the equilibrium state $\boldsymbol{b}^{\infty}$ is defined such that the models converge to the same asymptotic solution. For this, $\boldsymbol{b}^{\infty}$ is defined as the representation (3.4) with the coefficients given by (4.10). In the relaxation model proposed by Speziale &

Xu (1996), the expression for the relaxation coefficient C, consistent with the Crow constraint (Speziale & Xu 1996), is given by

$$C = \frac{8}{15}\frac{1}{B_1^S}, \tag{5.4}$$

where $B_1^S = 0.3326$ is the equilibrium value of the representation coefficient B_1 in (3.4) for a strained flow, using the SSG pressure–strain rate model coefficients. This guarantees that the early time behaviour of the relaxation of the anisotropy is well captured in an initially isotropic turbulence subjected to a mild strain. The relaxation model proposed by Girimaji (1999*a*) can also be cast in the present formalism, with the relaxation coefficient defined as

$$C = \frac{\eta_\infty}{\eta_\infty - \eta}\frac{\mathrm{d}\eta}{\mathrm{d}t^*}. \tag{5.5}$$

With this expression for the relaxation coefficient, the scalar function appearing in (5.2) is easily evaluated

$$\exp\left(-\int_0^{t^*}\frac{C}{\eta}\,\mathrm{d}s\right) = \left|\frac{\eta_\infty - \eta(t^*)}{\eta_\infty - \eta_0}\right|\frac{\eta_0}{\eta(t^*)}. \tag{5.6}$$

Therefore, it is evident that this type of relaxation model leads to a restricted evolution pattern for the stress anisotropy tensor, since (5.2) and (5.6) give

$$\boldsymbol{b}(t^*) = \left[1 - \left|\frac{\eta_\infty - \eta(t^*)}{\eta_\infty - \eta_0}\right|\frac{\eta_0}{\eta(t^*)}\right]\boldsymbol{b}^\infty + \left|\frac{\eta_\infty - \eta(t^*)}{\eta_\infty - \eta_0}\right|\frac{\eta_0}{\eta(t^*)}\boldsymbol{b}_0. \tag{5.7}$$

According to Girimaji (1999*a*), the underlying motivation for this model is to generalize the equilibrium assumption $\mathrm{d}\boldsymbol{b}/\mathrm{d}t^* \sim 0$ on which algebraic stress closures are based (Gatski & Speziale 1993). Written in the phase-space, the approximation corresponds to the assumption

$$\frac{\mathrm{d}\boldsymbol{b}}{\mathrm{d}(1/\eta)} \sim \frac{\boldsymbol{b} - \boldsymbol{b}^\infty}{(1/\eta) - (1/\eta_\infty)}, \tag{5.8}$$

which is assumed to model the 'slow-manifold' stage of the anisotropy evolution toward the fixed point (Girimaji 1999*a*). But in this case, a simple integration of (5.8) (or a rearrangement of equation (5.7)) shows that the evolution of the stress anisotropy in the phase-space is constrained to the curve

$$\boldsymbol{b} - \boldsymbol{b}^\infty = \left|\frac{1/\eta - 1/\eta_\infty}{1/\eta_0 - 1/\eta_\infty}\right|(\boldsymbol{b}_0 - \boldsymbol{b}^\infty), \tag{5.9}$$

corresponding to straight lines connecting the initial state $(1/\eta_0, \boldsymbol{b}_0)$ to the equilibrium state $(1/\eta_\infty, \boldsymbol{b}^\infty)$ in the $(1/\eta, \boldsymbol{b})$-plane.

Beside the limited validity of this hypothesis, this type of relaxation model may lead to a fundamental stability problem when coupled with an evolution equation for η such as (3.22). For positive values of the relaxation coefficient C, as for instance in the Speziale & Xu (1996) model, the simple linear combination in (5.2) always gives bounded anisotropy values, lying between the initial anisotropy state $\boldsymbol{b}_0$ and the equilibrium state $\boldsymbol{b}^\infty$, and the relaxation model is well-behaved. But when the relaxation coefficient is allowed to take negative values, the anisotropy tensor may grow unbounded. Consider for instance the case where C is defined as in (5.5). With

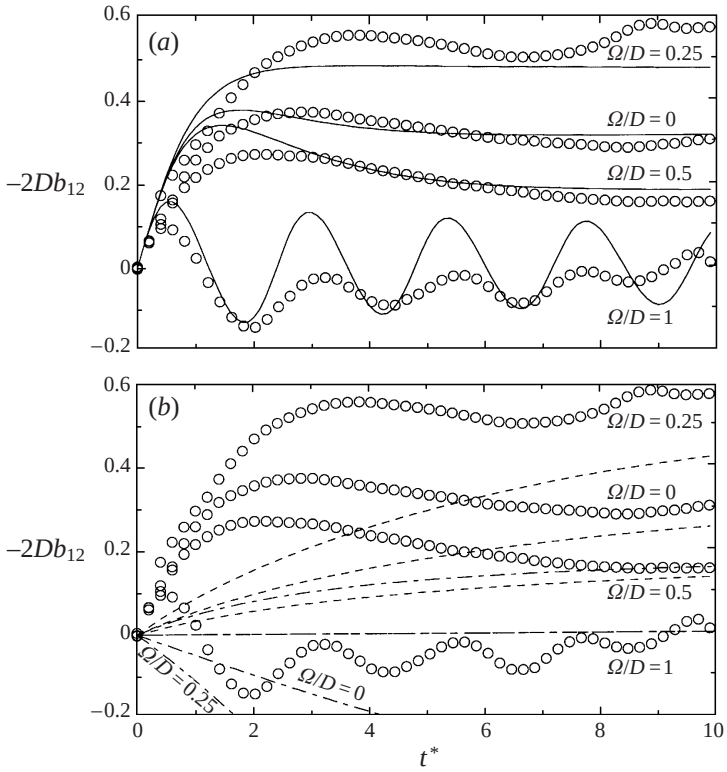

FIGURE 10. Time evolution of the normalised production $\mathscr{P}/K = -2Db_{12}$ for a homogeneous shear subjected to a solid-body rotation. (*a*) ———, Present non-equilibrium model. (*b*) – – –, Non-equilibrium relaxation model (Speziale & Xu 1996); – · – ·, non-equilibrium relaxation model (Girimaji 1999*a*). For both figures: ○, DNS (Tanaka *et al.* 1997).

(5.6), it is easy to show that

$$\exp\left(-\int_0^{t^*} \frac{C}{\eta}\mathrm{d}s\right) > 1 \quad \text{for} \quad \eta > \eta_0 > \eta_\infty. \tag{5.10}$$

Starting from an isotropic turbulence ($\boldsymbol{b}_0 = 0$), the normalised strain rate will initially grow, according to equation (3.22) rewritten as

$$\frac{\mathrm{d}\eta}{\mathrm{d}t^*} = (C_{\varepsilon 1} - 1)\left[\left(\frac{\mathscr{P}}{\varepsilon}\right)_\infty - \frac{\mathscr{P}}{\varepsilon}\right], \tag{5.11}$$

where the initial production-to-dissipation ratio is 0 (with $C_{\varepsilon 1} > 1$ and $C_{\varepsilon 2} > 1$, as is virtually always the case). For cases where $\eta_0 > \eta_\infty$, the factor in front of $\boldsymbol{b}^\infty$ in (5.2) will then be negative, leading to a negative production-to-dissipation ratio. In this case, $\mathrm{d}\eta/\mathrm{d}t^* > 0$, and the normalised strain rate will further increase, leading finally to an unbounded growth of the whole system.

As a first illustration of the performances of these various non-equilibrium models, consider a uniformly sheared flow ($\omega = D$) subjected to a solid-body rotation. As pointed out by Speziale *et al.* (1996), single-point closures are able to correctly delimit the stability boundaries of such flows consistent with RDT theory (Cambon *et al.* 1994). The predictions of the present non-equilibrium model are compared to the recent direct numerical simulation (DNS) results of Tanaka *et al.* (1997). Four rotation

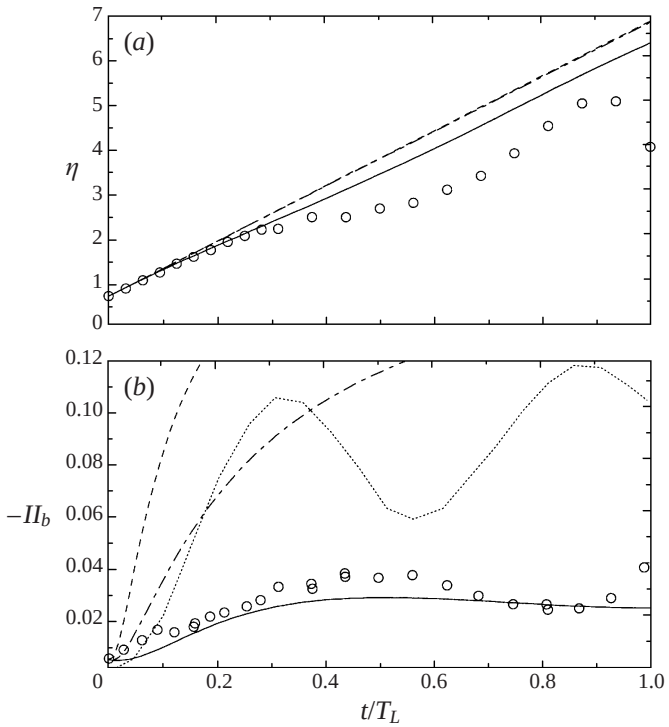

FIGURE 11. (*a*) Time evolution of the normalised strain rate η; (*b*) time evolution of the second invariant of the anisotropy tensor. ———, Present non-equilibrium model; – – –, non-equilibrium relaxation model (Speziale & Xu 1996); – · – ·, non-equilibrium relaxation model (Girimaji 1999); · · · ·, RDT solution (only shown for (*b*)); ○, experiments (Leuchter *et al.* 1992).

regimes are considered: $\Omega/D = 0, 0.25, 0.5$, and 1, and the corresponding values of the flow parameter $|\mathscr{R}|$ are, respectively, $|\mathscr{R}| = 1, 0.125, 1.25$, and 3.5, for the SSG pressure–strain rate correlation c_w values. The initial turbulence is isotropic, with $\eta_0 \approx 5.66$. Figure 10 shows the time evolution of the normalised production $\mathscr{P}/K = -2Db_{12}$ for the different rotation regimes. The same evolution is also plotted in figure 10 for the relaxation models in (5.1) with the relaxation coefficient defined by (5.4) or by (5.5). Unfortunately, in the latter case, the model is unstable in the two rotation regimes $\Omega/D = 0$ and 0.25, since according to equation (4.14), $\eta_\infty = 4.27$ and 2.85, respectively. For these two cases, $\eta_0 > \eta_\infty$, and the Girimaji (1999*a*) relaxation model is not stable, for the reasons discussed above. This can be seen in figure 10, where the value of $\mathscr{P}/K$ goes to $-\infty$ in this case. For the other cases, while the long-time solutions predicted by the present non-equilibrium model and the relaxation models are identical, the initial behaviour is radically different. The relaxation models lead to shear stress anisotropy evolutions that differ significantly from the experimental ones, while the present non-equilibrium model is able to capture the initial trends, including the strongly rotating case, for which the production $-2Db_{12}$ oscillates and takes negative values, which contributes to the rapid decay of turbulence. The relaxation models incorrectly predict $b_{12} = 0$ for this rotation regime, simply because $b_{12}^\infty = b_{12}(0) = 0$. Due to this inherent limitation, the relaxation models are unable to reproduce any limit-cycle behaviour.

As a second illustration, consider the case of homogeneous turbulence subjected to a rotation-dominated plane distortion. The mean velocity gradients are defined by

(3.23), with $\omega/D = 2$ and $D = 31.4\,\mathrm{s}^{-1}$. Such elliptic flows are also characterised by the aspect ratio $E = [(\omega + D)/(\omega - D)]^{1/2}$ of the mean flow streamline pattern. Here, the reference frame is inertial ($\Omega = 0$), and the corresponding value of $\mathscr{R}$ is 2 and E is $\sqrt{3}$. As pointed out by Leuchter, Benoit & Cambon (1992), as $\omega > D$, the Lagrangian displacement gradient tensor associated with the velocity field is periodic in time, with a period $2\pi(\omega^2 - D^2)^{-1/2}$. In the experiment of Leuchter *et al.* (1992), the turbulence at the beginning of the distorting section is slightly anisotropic, with an axisymmetric component ($b_{11} = -0.041$, $b_{22} = -0.043$, $b_{33} = 0.084$, and $b_{12} = -0.011$). The corresponding experimental value of DK_0/ε_0 is as low as 0.527, leading to $\eta_0 = 0.745$. Since for this homogeneous flow configuration, $\mathscr{R} > \mathscr{R}_{\mathrm{lim}}$, the normalised strain rate η will grow unbounded, and the time evolution of the anisotropy will have an oscillatory character. This is illustrated on figure 11, where the evolution of η is shown over one period of the mean velocity deformation. Since the initial value of η is very small, the oscillations will undergo a fast initial damping, as explained in a previous section, and illustrated in figure 7. The time evolution of the second invariant of the Reynolds stress anisotropy, II_b, is also shown in figure 11 for the present non-equilibrium model and for the relaxation models. For comparison, results from RDT are also shown (see Leuchter *et al.* 1992). These results are encouraging since it has been shown that even in this (weak) elliptic flow single-point closures can still predict qualitative features of the turbulence. Nevertheless, it should be expected that stronger elliptic flows with lower aspect ratios E will yield poorer predictions for both the full differential Reynolds stress model and the algebraic stress model.

The present non-equilibrium model is able to reproduce the main features of the evolution of II_b, whereas the undulations of the RDT solution are much more pronounced than in the experiments, with a higher amplitude and shorter wavelength, obviously a consequence of the low value of the normalised strain rate η and of neglecting the nonlinear damping effects in the calculations (Leuchter *et al.* 1992). The relaxation models do not capture any oscillation, and show a too rapid increase.

6. Conclusions

A general procedure has been developed that allows the investigation of the time evolution of the Reynolds stress anisotropy components in all planar homogeneous turbulent flows. The procedure takes the evolution equation for the Reynolds stress anisotropy tensor and replaces it with an equivalent system of equations for characteristic scalar invariants. This equivalent system can then be used for assessing the dynamical behaviour of a variety of turbulence closure models. This includes pressure–strain rate models which are quadratic (or higher) in the anisotropy tensor and in which other anisotropic effects, such as dissipation rate anisotropy, can be taken into account. For the case of quasi-linear pressure–strain rate models, the system of ordinary differential equations can be analytically integrated when the relative strain parameter is assumed to vary slowly, and an explicit expression can be found for the time evolution of the anisotropy of the Reynolds stress tensor in all planar homogeneous flows. The present non-equilibrium solution accurately predicts both the initial behaviour of the modelled Reynolds stress evolution, and the asymptotic equilibrium states. With this solution, the full dynamic behaviour of the Reynolds stresses has been investigated, including effects of initial states, early time evolution, limit-cycle occurrence, and existence and global stability of the asymptotic states. In addition, it has been demonstrated that the Reynolds stress invariants are uniquely determined by the model closure coefficients, independent of any explicit dependence

on the mean deformation field. Constraints for the development of more general and realizable pressure–strain rate correlation models have also been determined. A non-equilibrium stress model has been derived from the analytic temporal solution of the Reynolds stress anisotropies, and has been shown to outperform recently proposed relaxation models in temporally evolving homogeneous flows.

The first author acknowledges the financial support from the Commission Suisse pour l'Encouragement de la Recherche Scientifique, and the support of Sulzer Brothers S.A. under contract number 3062.1. The authors would also like to thank Dr O. Leuchter for providing them with the initial conditions used in his experiments, and express their gratitude to Professor M. O. Deville for the helpful discussions and particularly the comments concerning the organization of Appendix C.

Appendix A. Representation of $\boldsymbol{b}^2 - \frac{1}{3}\{\boldsymbol{b}^2\}\boldsymbol{I}$

Consider a symmetric, traceless tensor $\boldsymbol{b}$ for which the elements in any rectangular coordinate system are functions of the elements of two independent traceless tensors $\boldsymbol{S}^*$ (symmetric) and $\boldsymbol{W}^*$ (antisymmetric) in the same coordinate system, which is written as

$$b_{ij} = b_{ij}(S^*_{kl}, W^*_{kl}).$$

The forms of these functional relationships also must be independent of the particular coordinate system in which they are expressed; that is, the relation between $\boldsymbol{b}$, $\boldsymbol{S}^*$, and $\boldsymbol{W}^*$ is isotropic (Rivlin & Ericksen 1955).

For two-dimensional mean flows, $\boldsymbol{S}^*$ has one vanishing eigenvalue, and in the principal coordinate system of $\boldsymbol{S}^*$, the vorticity vector is aligned with the eigenvector of $\boldsymbol{S}^*$ that corresponds to the vanishing eigenvalue. If the tensor $\boldsymbol{b}^*$ is also assumed to have one eigenvector aligned with the eigenvector of $\boldsymbol{S}^*$ that corresponds to the vanishing eigenvalue, then the tensor $\boldsymbol{b}$ can be represented in terms of the tensors $\boldsymbol{S}^*$ and $\boldsymbol{W}^*$ and the scalar invariants $\{\boldsymbol{bS}^*\}$, $\{\boldsymbol{bW}^*\boldsymbol{S}^*\}$, and $\{\boldsymbol{bS}^{*2}\}$, as (see Jongen & Gatski 1998*b*)

$$\boldsymbol{b} = \{\boldsymbol{bS}^*\}\boldsymbol{S}^* + \frac{\{\boldsymbol{bW}^*\boldsymbol{S}^*\}}{\{\boldsymbol{W}^{*2}\}}(\boldsymbol{S}^*\boldsymbol{W}^* - \boldsymbol{W}^*\boldsymbol{S}^*) + 6\{\boldsymbol{bS}^{*2}\}\left(\boldsymbol{S}^{*2} - \tfrac{1}{3}\boldsymbol{I}\right). \tag{A 1}$$

The quadratic term $\boldsymbol{b}^2 - \frac{1}{3}\{\boldsymbol{b}^2\}\boldsymbol{I}$ can also be represented in terms of the tensors $\boldsymbol{S}^*$ and $\boldsymbol{W}^*$ and the scalar invariants $\{\boldsymbol{bS}^*\}$, $\{\boldsymbol{bW}^*\boldsymbol{S}^*\}$, and $\{\boldsymbol{bS}^{*2}\}$.

If in expression (A 1) the symmetric, traceless tensor $\boldsymbol{b}$ is replaced by $\boldsymbol{b}^2 - \frac{1}{3}\{\boldsymbol{b}^2\}\boldsymbol{I}$, then the following equation is obtained:

$$\begin{aligned}\boldsymbol{b}^2 - \tfrac{1}{3}\{\boldsymbol{b}^2\}\boldsymbol{I} = \{\boldsymbol{b}^2\boldsymbol{S}^*\}\boldsymbol{S}^* + \frac{\{\boldsymbol{b}^2\boldsymbol{W}^*\boldsymbol{S}^*\}}{\{\boldsymbol{W}^{*2}\}}(\boldsymbol{S}^*\boldsymbol{W}^* - \boldsymbol{W}^*\boldsymbol{S}^*) \\ +6\left(\{\boldsymbol{b}^2\boldsymbol{S}^{*2}\} - \tfrac{1}{3}\{\boldsymbol{b}^2\}\right)\left(\boldsymbol{S}^{*2} - \tfrac{1}{3}\boldsymbol{I}\right).\end{aligned} \tag{A 2}$$

Now, the scalar invariants $\{\boldsymbol{b}^2\boldsymbol{S}^*\}$, $\{\boldsymbol{b}^2\boldsymbol{W}^*\boldsymbol{S}^*\}$, and $\{\boldsymbol{b}^2\boldsymbol{S}^{*2}\}$ in (A 2) must be expressed in terms of the scalar invariants $\{\boldsymbol{bS}^*\}$, $\{\boldsymbol{bW}^*\boldsymbol{S}^*\}$, and $\{\boldsymbol{bS}^{*2}\}$.

For conciseness, relation (A 1) can be rewritten as

$$\boldsymbol{b} = \sum_{i=1}^{3} \alpha_i \boldsymbol{T}_i, \tag{A 3}$$

where the scalar coefficients α_i are

$$\alpha_1 = \{\boldsymbol{b}\boldsymbol{S}^*\}, \qquad \alpha_2 = \{\boldsymbol{b}\boldsymbol{W}^*\boldsymbol{S}^*\}/\{\boldsymbol{W}^{*2}\}, \qquad \alpha_3 = 6\{\boldsymbol{b}\boldsymbol{S}^{*2}\}, \tag{A 4}$$

and the tensors $\boldsymbol{T}_i$ are given by

$$\boldsymbol{T}_1 = \boldsymbol{S}^*, \qquad \boldsymbol{T}_2 = \boldsymbol{S}^*\boldsymbol{W}^* - \boldsymbol{W}^*\boldsymbol{S}^*, \qquad \boldsymbol{T}_3 = \boldsymbol{S}^{*2} - \tfrac{1}{3}\boldsymbol{I}. \tag{A 5}$$

Therefore,

$$\{\boldsymbol{b}^2\boldsymbol{S}^*\} = \{\boldsymbol{b}^2\boldsymbol{T}_1\}, \qquad \{\boldsymbol{b}^2\boldsymbol{W}^*\boldsymbol{S}^*\} = -\tfrac{1}{2}\{\boldsymbol{b}^2\boldsymbol{T}_2\}, \qquad \{\boldsymbol{b}^2\boldsymbol{S}^{*2}\} - \tfrac{1}{3}\{\boldsymbol{b}^2\} = \{\boldsymbol{b}^2\boldsymbol{T}_3\},$$

and if (A 3) is inserted into the above expressions, then

$$\{\boldsymbol{b}^2\boldsymbol{T}_i\} = \sum_{j=1}^{3}\sum_{k=1}^{3}\alpha_j\alpha_k\{\boldsymbol{T}_j\boldsymbol{T}_k\boldsymbol{T}_i\} \quad (i = 1, 2, 3). \tag{A 6}$$

Finally, the 27 invariants $\{\boldsymbol{T}_j\boldsymbol{T}_k\boldsymbol{T}_i\}$, $(i, j, k = 1, 2, 3)$ must be evaluated. As a result of symmetry properties $((j,k,i) = (i,j,k) = (k,i,j))$, only 11 invariants must be computed: $(i,j,k) = (1,1,1)$, $(1,1,2)$, $(1,1,3)$, $(1,2,2)$, $(1,2,3)$, $(1,3,2)$, $(1,3,3)$, $(2,2,2)$, $(2,2,3)$, $(2,3,3)$, and $(3,3,3)$. With the generalised version of the Cayley–Hamilton theorem (Spencer & Rivlin 1959), the only resulting non-zero invariants are

$$\{\boldsymbol{T}_1^2\boldsymbol{T}_3\} = \tfrac{1}{6}, \qquad \{\boldsymbol{T}_2^2\boldsymbol{T}_3\} = -\tfrac{1}{3}\{\boldsymbol{W}^{*2}\}, \qquad \{\boldsymbol{T}_3^3\} = -\tfrac{1}{36},$$

together with the invariants that result from the cyclic permutations of the indices. Therefore, the relations

$$\left.\begin{aligned}
\{\boldsymbol{b}^2\boldsymbol{S}^*\} &= \tfrac{1}{3}\alpha_1\alpha_3 = 2\{\boldsymbol{b}\boldsymbol{S}^*\}\{\boldsymbol{b}\boldsymbol{S}^{*2}\},\\
\{\boldsymbol{b}^2\boldsymbol{W}^*\boldsymbol{S}^*\} &= \tfrac{1}{3}\alpha_2\alpha_3\{\boldsymbol{W}^{*2}\} = 2\{\boldsymbol{b}\boldsymbol{W}^*\boldsymbol{S}^*\}\{\boldsymbol{b}\boldsymbol{S}^{*2}\},\\
\{\boldsymbol{b}^2\boldsymbol{S}^{*2}\} - \tfrac{1}{3}\{\boldsymbol{b}^2\} &= \tfrac{1}{6}\alpha_1^2 - \tfrac{1}{3}\alpha_2^2\{\boldsymbol{W}^{*2}\} - \tfrac{1}{36}\alpha_3^2 = \tfrac{1}{6}\{\boldsymbol{b}\boldsymbol{S}^*\}^2 - \frac{1}{3}\frac{\{\boldsymbol{b}\boldsymbol{W}^*\boldsymbol{S}^*\}^2}{\{\boldsymbol{W}^{*2}\}} - \{\boldsymbol{b}\boldsymbol{S}^{*2}\}^2,
\end{aligned}\right\} \tag{A 7}$$

lead to the desired expression for the quadratic term in (3.2).

Appendix B. Derivation of $\{\boldsymbol{b}\boldsymbol{S}^*\}$, $\{\boldsymbol{b}\boldsymbol{W}^*\boldsymbol{S}^*\}$, and $\{\boldsymbol{b}\boldsymbol{S}^{*2}\}$ equations

Starting from the tensor evolution equation for the Reynolds stress anisotropy (2.11), a system of three scalar ordinary differential equations in the three scalar unknowns $\{\boldsymbol{b}\boldsymbol{S}^*\}$, $\{\boldsymbol{b}\boldsymbol{W}^*\boldsymbol{S}^*\}$, and $\{\boldsymbol{b}\boldsymbol{S}^{*2}\}$ can be derived.

By multiplying relation (2.11) by $\boldsymbol{S}^*$, taking the trace of the equation, and using the results of Appendix A to express $\{\boldsymbol{b}^2\boldsymbol{S}^*\}$ in terms of $\{\boldsymbol{b}\boldsymbol{S}^*\}$ and $\{\boldsymbol{b}\boldsymbol{S}^{*2}\}$, the following equation is obtained:

$$\left\{\frac{\mathrm{d}\boldsymbol{b}}{\mathrm{d}t^*}\boldsymbol{S}^*\right\} = -\frac{a_0}{\eta}\{\boldsymbol{b}\boldsymbol{S}^*\} - 2a_3\{\boldsymbol{b}\boldsymbol{S}^{*2}\} + 2a_2\{\boldsymbol{b}\boldsymbol{W}^*\boldsymbol{S}^*\} + \frac{2a_4}{\eta}\{\boldsymbol{b}\boldsymbol{S}^*\}\{\boldsymbol{b}\boldsymbol{S}^{*2}\} - a_1 - \{\boldsymbol{L}^*\boldsymbol{S}^*\}. \tag{B 1}$$

Similarly, multiplying equation (2.11) by either $\boldsymbol{W}^*\boldsymbol{S}^*$ or $\boldsymbol{S}^{*2}$ and taking the trace of the equation leads to the following equations, respectively:

$$\left\{\frac{\mathrm{d}\boldsymbol{b}}{\mathrm{d}t^*}\boldsymbol{W}^*\boldsymbol{S}^*\right\} = -\frac{a_0}{\eta}\{\boldsymbol{b}\boldsymbol{W}^*\boldsymbol{S}^*\} - a_2\frac{\zeta^2}{\eta^2}\{\boldsymbol{b}\boldsymbol{S}^*\} + \frac{2a_4}{\eta}\{\boldsymbol{b}\boldsymbol{W}^*\boldsymbol{S}^*\}\{\boldsymbol{b}\boldsymbol{S}^{*2}\} - \{\boldsymbol{L}^*\boldsymbol{W}^*\boldsymbol{S}^*\}, \tag{B 2}$$

and

$$\left\{\frac{\mathrm{d}\boldsymbol{b}}{\mathrm{d}t^*}\boldsymbol{S}^{2*}\right\} = -\frac{a_0}{\eta}\{\boldsymbol{b}\boldsymbol{S}^{*2}\} - \tfrac{1}{3}a_3\{\boldsymbol{b}\boldsymbol{S}^*\} + \tfrac{1}{6}a_4\{\boldsymbol{b}\boldsymbol{S}^*\}^2 + \frac{a_4}{3\eta}\frac{\eta^2}{\zeta^2}\{\boldsymbol{b}\boldsymbol{W}^*\boldsymbol{S}^*\}^2 - \frac{a_4}{\eta}\{\boldsymbol{b}\boldsymbol{S}^{*2}\}^2 - \{\boldsymbol{L}^*\boldsymbol{S}^{*2}\}. \quad \text{(B 3)}$$

In obtaining these two equations, the following relations are used:

$$\{\boldsymbol{b}\boldsymbol{S}^{*3}\} = \tfrac{1}{2}\{\boldsymbol{b}\boldsymbol{S}^*\}, \qquad 2\{\boldsymbol{b}\boldsymbol{W}^{*2}\boldsymbol{S}^*\} + \{\boldsymbol{b}\boldsymbol{W}^*\boldsymbol{S}^*\boldsymbol{W}^*\} = -\frac{1}{2}\frac{\zeta^2}{\eta^2}\{\boldsymbol{b}\boldsymbol{S}^*\},$$

which are consequences of the Cayley–Hamilton theorem (Spencer & Rivlin 1959). Because the velocity gradients have been assumed independent of time, the following relations hold:

$$\left\{\frac{\mathrm{d}\boldsymbol{b}}{\mathrm{d}t^*}\boldsymbol{S}^*\right\} = \frac{\mathrm{d}}{\mathrm{d}t^*}\{\boldsymbol{b}\boldsymbol{S}^*\}, \quad \left\{\frac{\mathrm{d}\boldsymbol{b}}{\mathrm{d}t^*}\boldsymbol{W}^*\boldsymbol{S}^*\right\} = \frac{\mathrm{d}}{\mathrm{d}t^*}\{\boldsymbol{b}\boldsymbol{W}^*\boldsymbol{S}^*\}, \quad \left\{\frac{\mathrm{d}\boldsymbol{b}}{\mathrm{d}t^*}\boldsymbol{S}^{2*}\right\} = \frac{\mathrm{d}}{\mathrm{d}t^*}\{\boldsymbol{b}\boldsymbol{S}^{*2}\}. \quad \text{(B 4)}$$

Equations (B 1), (B 2), and (B 3) lead, therefore, to the desired system of scalar ordinary differential equations for the invariants $\{\boldsymbol{b}\boldsymbol{S}^*\}$, $\{\boldsymbol{b}\boldsymbol{W}^*\boldsymbol{S}^*\}$, and $\{\boldsymbol{b}\boldsymbol{S}^{*2}\}$,

$$\frac{\mathrm{d}}{\mathrm{d}t^*}\{\boldsymbol{b}\boldsymbol{S}^*\} = -\frac{a_0}{\eta}\{\boldsymbol{b}\boldsymbol{S}^*\} - 2a_3\{\boldsymbol{b}\boldsymbol{S}^{*2}\} + 2a_2\{\boldsymbol{b}\boldsymbol{W}^*\boldsymbol{S}^*\} - a_1 - \{\boldsymbol{L}^*\boldsymbol{S}^*\} + \frac{2a_4}{\eta}\{\boldsymbol{b}\boldsymbol{S}^*\}\{\boldsymbol{b}\boldsymbol{S}^{*2}\}, \quad \text{(B 5)}$$

$$\frac{\mathrm{d}}{\mathrm{d}t^*}\{\boldsymbol{b}\boldsymbol{W}^*\boldsymbol{S}^*\} = -\frac{a_0}{\eta}\{\boldsymbol{b}\boldsymbol{W}^*\boldsymbol{S}^*\} - a_2\frac{\zeta^2}{\eta^2}\{\boldsymbol{b}\boldsymbol{S}^*\} - \{\boldsymbol{L}^*\boldsymbol{W}^*\boldsymbol{S}^*\} + \frac{2a_4}{\eta}\{\boldsymbol{b}\boldsymbol{W}^*\boldsymbol{S}^*\}\{\boldsymbol{b}\boldsymbol{S}^{*2}\}, \quad \text{(B 6)}$$

$$\frac{\mathrm{d}}{\mathrm{d}t^*}\{\boldsymbol{b}\boldsymbol{S}^{*2}\} = -\frac{a_0}{\eta}\{\boldsymbol{b}\boldsymbol{S}^{*2}\} - \tfrac{1}{3}a_3\{\boldsymbol{b}\boldsymbol{S}^*\} - \{\boldsymbol{L}^*\boldsymbol{S}^{*2}\} + \frac{a_4}{6\eta}\{\boldsymbol{b}\boldsymbol{S}^*\}^2 + \frac{a_4}{3\eta}\frac{\eta^2}{\zeta^2}\{\boldsymbol{b}\boldsymbol{W}^*\boldsymbol{S}^*\}^2 - \frac{a_4}{\eta}\{\boldsymbol{b}\boldsymbol{S}^{*2}\}^2. \quad \text{(B 7)}$$

Appendix C. Solution of anisotropy evolution equation

The change of variables

$$B_1 = \psi, \quad \text{(C 1)}$$

$$B_2 = \frac{a_3}{a_2}\zeta - \frac{a_2\mathscr{R}^2}{H}\phi, \quad \text{(C 2)}$$

$$B_3 = \zeta - \frac{a_3}{3H}\phi, \quad \text{(C 3)}$$

transforms system (3.6) into the quadratic system of ordinary differential equations

$$\dot{\zeta} = \left(2\alpha\psi - \beta/\eta\right)\zeta, \quad \text{(C 4)}$$

$$\dot{\phi} = \left(2\alpha\psi - \beta/\eta\right)\phi + H\psi, \quad \text{(C 5)}$$

$$\dot{\psi} = \left(2\alpha\psi - \beta/\eta\right)\psi + \phi - a_1, \quad \text{(C 6)}$$

where

$$H = \tfrac{2}{3}a_3^2 - 2a_2^2\mathscr{R}^2.$$

System (C 4)–(C 6) is subject to the following initial conditions:

$$\left.\begin{aligned} \psi_0 &= \psi(0) = B_{1,0}, \\ \phi_0 &= \phi(0) = 2a_2B_{2,0} - 2a_3B_{3,0}, \\ \zeta_0 &= \zeta(0) \;\; = \frac{1}{H}\left(\tfrac{2}{3}a_2a_3B_{2,0} - 2a_2^2\mathscr{R}^2B_{3,0}\right). \end{aligned}\right\} \tag{C 7}$$

The above relations are valid for $H \neq 0$. When $H = 0$, the differential system is singular, and another change of variables has to be considered. We will assume for the moment that $H \neq 0$, and will discuss the case $H = 0$ later. In the system (C 4)–(C 6), the evolution of the two variables ψ and ϕ is independent of the evolution of the variable ζ. Therefore, the quadratic system of ordinary differential equations

$$\dot{\phi} = -(\beta/\eta)\phi + H\psi + 2\alpha\psi\phi, \tag{C 8}$$

$$\dot{\psi} = -(\beta/\eta)\psi + \phi + 2\alpha\psi^2 - a_1, \tag{C 9}$$

can be solved, and the evolution of ζ is deduced by integrating (C 4),

$$\zeta(t^*) = \zeta_0 \exp\int_0^{t^*}\left[2\alpha\psi(s) - \frac{\beta}{\eta(s)}\right]\mathrm{d}s. \tag{C 10}$$

Equation (C 8) is linear in ϕ and, after integration, the evolution of ϕ is given as a function of ψ,

$$\phi(t^*) = H\exp\left(\int_0^{t^*}[2\alpha\psi(s) - \beta/\eta(s)]\,\mathrm{d}s\right)\int_0^{t^*}\psi(r)\exp\left(-\int_0^{r}[2\alpha\psi(s) - \beta/\eta(s)]\,\mathrm{d}s\right)\mathrm{d}r$$
$$+\phi_0\exp\left(\int_0^{t^*}[2\alpha\psi(s) - \beta/\eta(s)]\,\mathrm{d}s\right). \tag{C 11}$$

Equation (C 9) is, on the contrary, quadratic in ψ. It is a generalised Riccati equation (Davis 1962) which can be transformed into the homogeneous linear differential equation of second order

$$\ddot{\omega} = \beta\frac{\dot{\omega}}{\eta} - 2\alpha(\phi - a_1)\omega \tag{C 12}$$

by introducing the transformation (Bender & Orszag 1978)

$$\psi(t^*) = -\frac{1}{2\alpha}\left(\frac{\dot{\omega}(t^*)}{\omega(t^*)} - \frac{\beta}{\eta(t^*)}\right). \tag{C 13}$$

Equation (C 11) for ϕ can be rewritten in terms of ω,

$$\phi(t^*) = -\frac{H}{2\alpha} + \frac{1}{2\alpha\omega(t^*)}\left[\omega(0)(H + 2\alpha\phi_0) + \beta H\int_0^{t^*}\frac{\omega(s)}{\eta(s)}\,\mathrm{d}s\right], \tag{C 14}$$

and inserted into equation (C 12). This leads to the following linear integro-differential equation:

$$\ddot{\omega} = \beta\frac{\dot{\omega}}{\eta} + \left(H + 2\alpha a_1 - \beta\frac{\dot{\eta}}{\eta^2}\right)\omega - \beta H\int_0^{t^*}\frac{\omega(s)}{\eta(s)}\mathrm{d}s - \omega(0)(H + 2\alpha\phi_0), \tag{C 15}$$

where $\omega(0)$ can take any non-zero value and $\dot{\omega}(0) = -\omega(0)(2\alpha\psi_0 - \beta/\eta_0) = -\omega(0)(2\alpha B_{1,0} - \beta/\eta_0)$, with $\eta_0 = \eta(0)$ as the initial value of the normalised strain rate. Finally, equation (C 15) is integrated with the following transformation

$$\Psi_1 = \int \omega/\eta, \qquad \Psi_2 = \dot{\Psi}_1 = \omega/\eta,$$
$$\Psi_3 = \dot{\Psi}_2 = \dot{\omega}/\eta + \omega(1\dot{/}\eta), \qquad \Psi_4 = \dot{\Psi}_3 = \ddot{\omega}/\eta + 2\dot{\omega}(1\dot{/}\eta) + \omega(1\ddot{/}\eta).$$

The functions Ψ_i are the solution of

$$\left.\begin{aligned} &\dot{\Psi}_1 = \Psi_2, \quad \dot{\Psi}_2 = \Psi_3, \\ &\dot{\Psi}_3 = -\frac{\beta}{\eta} H \Psi_1 + \left(H + 2\alpha a_1 - \frac{\ddot{\eta}}{\eta}\right)\Psi_2 + \frac{1}{\eta}(\beta - 2\dot{\eta})\Psi_3 - \frac{\eta_0}{\eta}\Psi_2(0)(H + H^0), \end{aligned}\right\} \tag{C 16}$$

where the initial conditions are given by $\Psi_1(0) = 0$, $\Psi_2(0) \neq 0$, and $\Psi_3(0) = -\Psi_2(0) \times (2\alpha B_{1,0} - \beta/\eta_0 - \dot{\eta}_0/\eta_0)$; and $H^0 = 2\alpha\phi_0 = 4\alpha(a_2 B_{2,0} - a_3 B_{3,0})$.

In the general case for which the normalised strain rate varies in time, system (C 16) is a linear system of ordinary differential equations with variable coefficients. In the case of slow variations of η, the approximations

$$\frac{\dot{\eta}}{\eta} \sim 0, \qquad \frac{\ddot{\eta}}{\eta} \sim 0 \tag{C 17}$$

are valid for not too small values of η. The system of ordinary differential equations (C 16) can then be solved using standard integration methods for systems of first-order differential linear equations with constant coefficients. After lengthy, but straightforward, computations the solution of the system (C 16) yields

$$\left.\begin{aligned} &\Psi_1(t^*) = \mathscr{C}\left[\sum_{r=1}^{3} p_r \frac{1}{\lambda_r} \mathrm{e}^{\lambda_r t^*} + p_0(H + H^0)\right], \\ &\Psi_2(t^*) = \mathscr{C}\sum_{r=1}^{3} p_r \mathrm{e}^{\lambda_r t^*}, \quad \Psi_3(t^*) = \mathscr{C}\sum_{r=1}^{3} p_r \lambda_r \mathrm{e}^{\lambda_r t^*}, \end{aligned}\right\} \tag{C 18}$$

where $\mathscr{C} = \Psi_2(0)[(\lambda_2 - \lambda_1)(\lambda_3 - \lambda_1)(\lambda_3 - \lambda_2)]^{-1}$ and

$$\left.\begin{aligned} &p_r = \left[\lambda_r^2 - 2\alpha B_{1,0}\lambda_r - (H + H^0)\right](\lambda_s - \lambda_q), \quad r = 1, 2, 3, \\ &p_0 = \frac{\lambda_3 - \lambda_2}{\lambda_1} + \frac{\lambda_1 - \lambda_3}{\lambda_2} + \frac{\lambda_2 - \lambda_1}{\lambda_3}. \end{aligned}\right\} \tag{C 19}$$

In (C 19), the indices q and s are chosen such that $e_{qrs} = -1$. The λ_r are eigenvalues that are obtained as roots of the following cubic characteristic polynomial:

$$\lambda^3 - \frac{\beta}{\eta}\lambda^2 - (H + 2\alpha a_1)\lambda + \frac{\beta}{\eta} H = 0. \tag{C 20}$$

Finally, in terms of the original variables $B_i(t^*)$, the explicit solution is

$$\left.\begin{aligned} B_1(t^*) &= \frac{1}{2\alpha}\left[\frac{\beta}{\eta(t^*)} - \frac{\Psi_3(t^*)}{\Psi_2(t^*)}\right], \\ B_2(t^*) &= \frac{a_2 \mathscr{R}^2}{2\alpha}\left[1 - \frac{\beta}{\eta(t^*)}\frac{\Psi_1(t^*)}{\Psi_2(t^*)} - \frac{\Psi_2(0)}{\Psi_2(t^*)}\right] + \frac{\Psi_2(0)}{\Psi_2(t^*)} B_{2,0}, \\ B_3(t^*) &= \frac{a_3}{6\alpha}\left[1 - \frac{\beta}{\eta(t^*)}\frac{\Psi_1(t^*)}{\Psi_2(t^*)} - \frac{\Psi_2(0)}{\Psi_2(t^*)}\right] + \frac{\Psi_2(0)}{\Psi_2(t^*)} B_{3,0}. \end{aligned}\right\} \tag{C 21}$$

In (C 21), the initial condition $\Psi_2(0) \neq 0$ is arbitrary, and its value can, therefore, be taken as $\Psi_2(0) = 1$.

In the above developments, it has been assumed that $H \neq 0$. When $H = 0$, another transformation of variables has to be considered:

$$B_1 = \psi, \qquad B_2 = \frac{a_3}{a_2}\phi + \frac{1}{2a_2}\zeta, \qquad B_3 = \phi, \tag{C 22}$$

which leads to the same differential equations as (C 4)–(C 6), except for the equation (C 5) for ϕ:

$$\dot{\phi} = \left(2\alpha\psi - \beta/\eta\right)\phi - \tfrac{1}{3}a_3\psi, \tag{C 23}$$

with the initial conditions

$$\psi_0 = B_{1,0}, \qquad \phi_0 = B_{3,0}, \qquad \zeta_0 = 2a_2B_{2,0} - 2a_3B_{3,0}. \tag{C 24}$$

It therefore follows that the solution procedure outlined above is still valid, and the same steps can be performed on the new system of ordinary differential equations in the new transformed variables (ψ, ϕ, ζ). At the end, the resulting expression for the solution in terms of the expansion coefficients B_i will still be given by equations (C 18)–(C 21), but with $H = 0$. In this case, one characteristic root of (C 20) vanishes, for example $\lambda_1 = 0$, and $\lambda_2 + \lambda_3 = \beta/\eta$. It is simple to show that even if in this case $p_0 \to \infty$ in (C 19), the characteristic functions Ψ_i, and therefore the representation coefficients B_i, remain bounded since

$$\lim_{\lambda_1 \to 0}\left[\frac{p_1}{\lambda_1}\mathrm{e}^{\lambda_1 t^*} + p_0H^0\right] = \left(2\alpha B_{1,0} - \frac{\lambda_2 + \lambda_3}{\lambda_2\lambda_3}H^0\right)(\lambda_3 - \lambda_2).$$

REFERENCES

Abid, R. & Speziale, C. G. 1993 Predicting equilibrium states with Reynolds stress closures in channel flow and homogeneous shear flow. *Phys. Fluids* A **5**, 1776–1782.

Bender, C. M. & Orszag, S. 1978 *Advanced Mathematical Methods for Scientist and Engineers.* McGraw-Hill.

Blaisdell, G. A. & Shariff, K. 1996 Simulation and modelling of the elliptic streamline flow. In *Proc. Summer Program, Center for Turbulence Research*, pp. 433–446. Stanford University.

Cambon, C., Benoit, J. P., Shao, L. & Jacquin, L. 1994 Stability analysis and large-eddy simulation of rotating turbulence with organised eddies. *J. Fluid Mech.* **278**, 175–200.

Cambon, C., Teissedre, C. & Jeandel, D. 1985 Étude d'effets couplés de déformation et de rotation sur une turbulence homogène. *J. Méc. Théo. Appl.* **4**, 629–657.

Davis, H. J. 1962 *Introduction to Nonlinear Differential and Integral Equations.* Dover.

Ferziger, J. H. 1993 Subgrid-scale modelling. In *Large-Eddy Simulation of Complex Engineering and Geophysical Flows* (ed. B. Galperin & S. A. Orszag), pp. 37–54. Cambridge University Press.

Gatski, T. B. & Speziale, C. G. 1993 On explicit algebraic stress models for complex turbulent flows. *J. Fluid Mech.* **254**, 59–78.

Gibson, M. M. & Launder, B. E. 1978 Ground effects on pressure fluctuations in the atmospheric boundary layer. *J. Fluid Mech.* **86**, 491–511.

Girimaji, S. S. 1996 Fully explicit and self-consistent algebraic Reynolds stress model. *Theor. Comput. Fluid Dyn.* **8**, 387–402.

Girimaji, S. S. 1997 Dynamical system analysis of Reynolds stress closure equations. In *Eleventh Symp. on Turbulent Shear Flows, Institut National Polytechnique de Grenoble – Université Joseph Fourier*.

Girimaji, S. S. 1999*a* Development of algebraic Reynolds stress model in non-equilibrium turbulence. In *Modeling Complex Turbulent Flows* (ed. M. Salas, J. N. Hefner & L. Sakell). Kluwer.

Girimaji, S. S. 1999*b* Pressure–strain correlation modelling of complex turbulent flows. Submitted to *J. Fluid Mech.*

Jongen, T. & Gatski, T. B. 1998*a* A new approach to characterizing the equilibrium states of the Reynolds stress anisotropy in homogeneous turbulence. *Theor. Comput. Fluid Dyn.* **11**, 31–47. Erratum: *Theor. Comput. Fluid Dyn.* **12**, 71–72.

Jongen, T. & Gatski, T. B. 1998*b* General explicit algebraic stress relations and best approximation for three-dimensional flows. *Intl J. Engng Sci.* **36**, 739–763.

Jongen, T., Mompean, G. & Gatski, T. B. 1998 Accounting for Reynolds stress and dissipation rate anisotropies in inertial and noninertial frames. *Phys. Fluids* **10**, 674–684.

Launder, B. E., Reece, G. & Rodi, W. 1975 Progress in the development of a Reynolds stress turbulence closure. *J. Fluid Mech.* **68**, 537–566.

Leuchter, O. & Benoit, J. P. 1991 Study of coupled effects of plane strain and rotation on homogeneous turbulence. In *Eighth Symp. on Turbulent Shear Flows, Technical University of Munich.*

Leuchter, O., Benoit, J. P. & Cambon, C. 1992 Homogeneous turbulence subjected to rotation-dominated plane distortion. In *Fourth European Turbulence Conf. Delft University of Technology.*

Lumley, J. L. 1978 Computational modelling of turbulent flows. *Adv. Appl. Mech.* **18**, 123–176.

Mansour, N. N., Shih, T.-H. & Reynolds, W. C. 1991 The effects of rotation on initially anisotropic homogeneous flows. *Phys. Fluids* A **3**, 2421–2425.

Reynolds, W. C. 1989 Effects of rotation on homogeneous turbulence. In *Proc. 10th Australian Fluid Mechanics Conference, University of Melbourne.*

Reynolds, W. C. & Kassinos, S. C. 1995 One-point modelling of rapidly deformed homogeneous turbulence. *Proc. R. Soc. Lond.* A **451**, 87–104.

Rivlin, R. S. & Ericksen, J. L. 1955 Stress-deformation relations for isotropic materials. *Arch. Rat. Mech. Anal.* **4**, 323–425.

Salhi, A. & Lili, T. 1996 Asymptotic analysis of equilibrium states for rotating turbulent flows. *Theor. Comput. Fluid Dyn.* **8**, 289–308.

Sarkar, S. & Speziale, C. G. 1990 A simple nonlinear model for the return to isotropy in turbulence. *Phys. Fluids* A **2**, 84–93.

Schumann, U. 1977 Realizability of Reynolds stress turbulence models. *Phys. Fluids* **20**, 721–725.

Spencer, A. J. M. & Rivlin, R. S. 1959 The theory of matrix polynomials and its application to the mechanics of isotropic continua. *Arch. Rat. Mech. Anal.* **2**, 309–336.

Speziale, C. G. 1998 Turbulence modelling for time-dependent RANS and VLES: a review. *AIAA J.* **36**, 173–184.

Speziale, C. G., Abid, R. & Blaisdell, G. A. 1996 On the consistency of Reynolds stress turbulence closures with hydrodynamic stability theory. *Phys. Fluids* **8**, 781–788.

Speziale, C. G., Abid, R. & Durbin, P. A. 1994 On the realizability of Reynolds stress turbulence closures. *J. Sci. Comput.* **9**, 369–403.

Speziale, C. G. & Mac Giolla Mhuiris, N. 1989 On the prediction of equilibrium states in homogeneous turbulence. *J. Fluid Mech.* **209**, 591–615.

Speziale, C. G., Sarkar, S. & Gatski, T. B. 1991 Modeling the pressure–strain correlation of turbulence: an invariant dynamical systems approach. *J. Fluid Mech.* **227**, 245–272.

Speziale, C. G. & Xu, X.-H. 1996 Towards the development of second-order closure models for non-equilibrium turbulent flows. *Intl J. Heat Fluid Flow* **17**, 238–244.

Tanaka, M., Yanase, S., Kida, S. & Kawahara, G. 1997 Uniformly sheared turbulent flow under the effect of solid-body rotation. In *Eleventh Symp. on Turbulent Shear Flows, Institut National Polytechnique de Grenoble – Université Joseph Fourier.*

Taulbee, D. B. 1992 An improved algebraic stress model and corresponding nonlinear stress model. *Phys. Fluids* A **4**, 2555–2561.

Ying, R. & Canuto, V. M. 1996 Turbulence modelling over two-dimensional hills using an algebraic Reynolds stress expression. *Boundary-Layer Met.* **77**, 69–99.